Final Colloquium

Benediktbeuern

September 29th - October 1st 2021

DFG PRIORITY PROGRAM 1681 MODELLIERUNG SYNTHESE ANWENDUNG SPP1681

Program Overview

Opening	29.09.2021	13:30 – 13:45
Medical Applications		13:45 – 15:45
Coffee Break		15:45 – 16:20
Complex Composites		16:20 – 18:10
Postersession		18:10 – 20:00
Walking / Bus Tour to Herzogstand	30.09.2021	08:45 – 16:00
Mountain Talks		
Ferrofluids & Technical Applications		16:30 – 18:30
Colloquium-Dinner		19:00 - …
Theory	01.10.2021	08:45 – 10:05
Coffee Break		10:05 – 10:30
Experimental Methods		10:30 – 12:30
Closing		12:30 – 12:40

next trains to Munich will leave 13:04 and 13:58

Content

18th FERROFLUIDWORKSHOP

Program of the Final Colloquium of DFG Priority Program 1681

Field controlled particle matrix interactions: synthesis, multiscale modelling and application of magnetic hybrid materials

and the ***18th German Ferrofluid Workshop***

Benediktbeuern, September 29th – October 1st 2021

Wednesday, September 29th

13:30 Opening

13:45 Medical applications

13:45	R. Stein, B. Friedrich, M. Mühlberger, N. Cebulla, E. Schreiber, R. Tietze, I. Cicha, C. Alexiou, S. Dutz, A. R. Boccaccini, H. Unterweger *Synthesis and Characterization of Citrate-Stabilized Gold-Coated SPIONs for Biomedical Applications*	59
14:05	D. Zahn, K. Klein, P. Radon, E. Nagel, M. Eichhorn, F. Wiekhorst, S. Dutz *Magnetic multicore nanoparticles for drug targeting to the eye*	72
14:25	L.J. Gresing, M. Sutter, P. Radon, A. Weidner, R.P. Friedrich, S. Dutz, C. Alexiou, F. Wiekhorst, A. Hochhaus, J.H. Clement *Magnetic nanoparticles pass an in vitro blood-placenta barrier under continuous flow conditions*	32
14:45	S. Dutz, A. Weidner, M. v.d. Lühe, C. Gräfe, P. Biehl, J. Demut, P. Warncke, S. Jungmann, D. Fischer, F.H. Schacher, J.H. Clement *Hybrid nanomaterials of biomolecule corona coated magnetic nanoparticles and their interaction with biological systems*	23
15:05	R. Müller, T. Heinze *Studies about the Design of Magnetic Bionanocomposite*	49
15:25	T. Viereck, F. Wolgast, M. Schilling, F. Ludwig *Low-cost Magnetic Particle Spectroscopy device for immunoassays*	67

15:45 Coffee Break & Posters

16:20 Complex Composites

16:20	M. Hähsler, S. Behrens *Surface engineering and stable dispersions of magnetic nanoparticles in a nematic liquid crystal*	34
16:40	M. Küster, H. Nádasi, N. Sebástian, P. H. Boštjančič, D. Lisjak, A. Mertelj, A. Eremin, F. Ludwig *Ferromagnetic nematics in rotating and oscillating magnetic fields*	39
17:00	L. Selzer, S. Odenbach *Rheological behavior of magnetic hydrogels*	57
17:20	A. Tschöpe, K. Birster, R. Schweitzer, C. Schopphoven *Field-Induced Deformation of Ferromagnetic Nanocomposites*	65
17:40	C. Czichy, S. Odenbach *Comparison of a practical and a theoretical approach to determine the bending curves of magnetic alginate hydrogel strings depending on particle concentration and aging*	21

18:10 Postersession

Thursday, September 30th

approx. 08:30 Mountain and Alternative Tour

Mountain Tour to Herzogstand

approx. 13:30 Mountain Talks

J. Landers	*Mössbauer spectroscopy applied to soft magnetic hybrid materials*
T. Scheibel	*Functionalization of biopolymer fibers with magnetic nanoparticles*

16:30 Ferrofluids & Technical Applications

19:00 Colloquium Dinner

Friday, October 1st

8:45 Theory

8:45	L. Fischer, A. M. Menzel *Magnetostriction of magnetic gels and elastomers – overall deformation based on a particle-resolved mesoscale description*	27
9:05	P. Gebhart, Th. Wallmersperger *Microstructure guided constitutive modeling of isotropic compressible magneto-active polymers at the macroscale level*	29
9:25	S. Goh, A. M. Menzel, R. Wittmann, H. Löwen *Density functional theory for a three-dimensional model of ferrogels*	30
9:45	K. A. Kalina, P. Metsch, M. Kästner *Continuum approaches for the modeling and simulation of magnetorheological elastomers*	36

10:05 Coffee Break & Posters

10:30 Experimental Methods

10:30	H. Schmidt, G. K. Auernhammer *Particle jumps in chains and lattices of magnetic particles*	51
10:50	P. Kreissl, Ch. Holm, R. Weeber *Studying the Coupling Mechanisms in Nano-Rheological Soft Magnetic Systems Using Computer Simulations*	37
11:10	J. Landers, M. Witt, J. Kopp, S. Hinrichs, S. Salamon, B. Hankiewicz, R. von Klitzing, H. Wende *Magnetic response of $CoFe_2O_4$ nanoparticles confined in PNIPAM-microgel networks*	41
11:30	D. Eberbeck, M. Kruteva, L. Fruhner, A. Feoktystov, R. Thiermann, A. Tschöpe, F. Wiekhorst *Evaluation of the determination of the core-shell structure of MNP and its opsonisation layer*	25
11:50	A.V. Bakhtiiarov, G.V. Stepanov, D.A. Lobanov, D.A. Semerenko *Alternating-current conductivity exhibited by magnetoactive elastomers with different fillers*	11
12:10	J. Seifert, K. Koch, M. Hess, A. M. Schmidt *Magneto-mechanical coupling of single domain particles in soft matter systems*	55

12:30 Closing

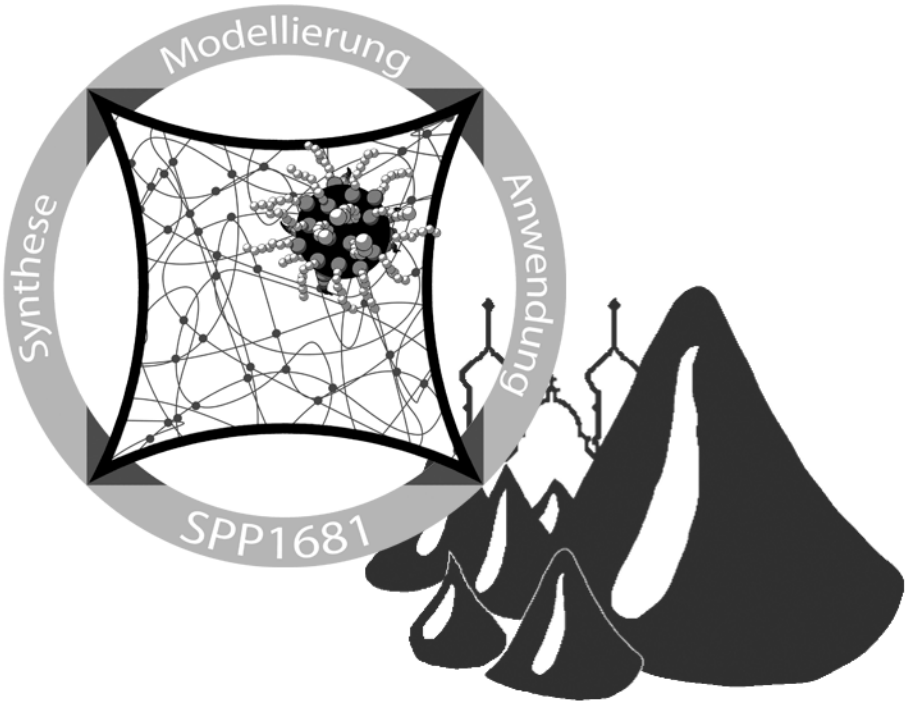

Abstracts

DFG PRIORITY PROGRAM 1681 M

18th FERROFLUIDWORKSHOP

Abstracts

On the ridge of instability in ferrofluidic Couette flow via alternating magnetic field

S. Altmeyer[1]

[1] *Castelldefels School of Telecom and Aerospace Engineering, Universitat Politècnica de Catalunya, 08034 Barcelona, Spain*

There is a huge number of natural and industrial flows, which are subjected to time-dependent boundary conditions. The flow of a magnetic fluid under the influence of temporal modulations is such an example. Here, we perform numerical simulations of ferrofluidic Couette flow [1, 2] subject to time-periodic modulation [3] in a spatially homogeneous magnetic field and report how such a modulation can lead to a significant Reynolds number Re enhancement. Consider the Taylor Couette system (TCS) [4] and a modified Niklas approximation [2, 3] we explain the relation between modulation amplitude, driving frequency and stabilization effect. From this, we describe the system response around the primary instability to be sensitive to an alternating field.

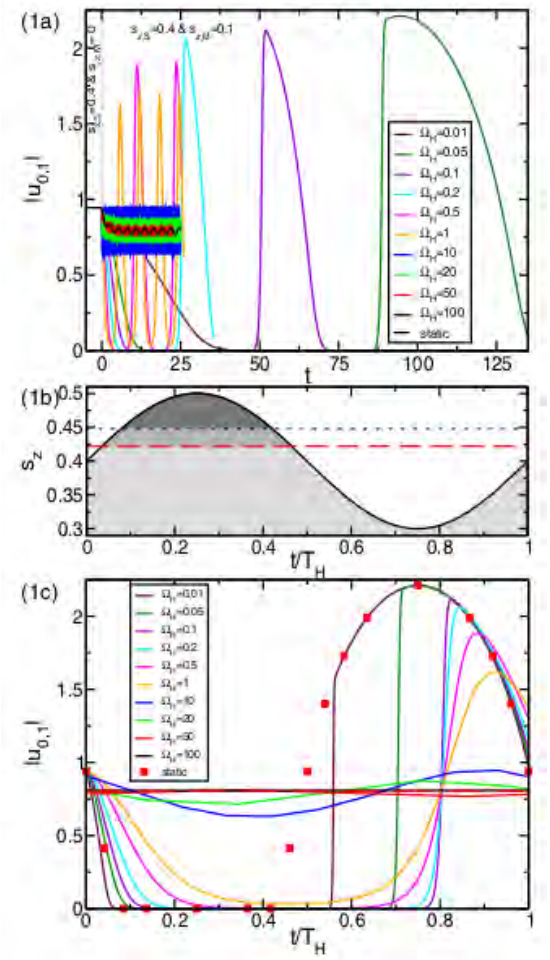

Figure 1: **Non-linear system response around the instability.** (a) Time evolution of the dominant mode amplitude $|u_{0,1}|$ as a function of time for different Ω_H as indicated and modulation amplitudes $s_{z,M} = 0.1$. (b) Temporal oscillations of the control function $s_z(t) = s_{z,S} + s_{z,M} \sin(\Omega_h t)$ ($s_{z,S} = 0.4$). (c) as (a) but as a function of the reduced time t/T_H. $Re = 80$. Red squares show the response to stationary magnetic field with magnetic field strength s_z given by the actual value of $s_z(t)$.

System setup

In the periodically modulated TCS, we give a sinusoidal modulation signal to the external magnetic field (parallel z-axis, uniform in space and harmonic in time) as $\mathbf{H}_z = [H_S + H_M \sin(\Omega_H t)]\mathbf{e}_z$. As earlier reported such a pure axial magnetic field *preserves* the system symmetries and only shift the stability thresholds [1, 5]. By using a modified Niklas approach [2, 1] the effect of the magnetic field and the magnetic properties of the ferrofluid on the velocity field can be characterized by the (time dependent) Niklas function [3]

$$s_z(t) = s_{z,S} + s_{z,M} \sin(\Omega_H t), \qquad (1)$$

with three control parameters, $s_{z,S}$ being the *static contribution*, $s_{z,M}$ the *modulation amplitude*, and Ω_H the *modulation frequency*.

Results

For parameters given in Fig. 1 the system becomes temporally subcritical for modulation amplitudes $s_{z,M} = 0.1$, while it *remains* slightly supercritical in pure static case ($s_{z,M} = 0.0$). In the high frequencies limit the time averaged magnetic field $\langle s_z(t)\rangle_T$ for modulated driving (dashed red line in Fig. 1(c)) corresponds to a static magnetic field with $s_{z,S} \approx 0.423$. With decreasing frequency Ω_H first the amplitude in the oscillating mode $|u_{0,1}|$ continuously increase before at $\Omega_H \lesssim 0.5$ it eventually becomes temporally *zero* indicating that the system is now subcritical. The smaller the frequency Ω_H, the longer the system remains subcritical (Fig. 1(c)). Over one period, for such low frequencies, a fast growth of the mode amplitude $|u_{0,1}|$ followed by a relaxing just similarly to values close to the stationary can be observed. With further decreasing Ω_H the oscillation profile in the mode amplitudes $|u_{0,1}|$ approaches the static scenario. In addition a temporally delay between the extrema of $s_z(t)$ and the corresponding extrema (min and max) in the mode amplitudes $|u_{0,1}|$ results from the inertia of the fluid resisting the fast changing accelerating Kelvin force and thus leading to this time lag.

Conclusion

We found that the system response is selective to driving parameters around the primary instability. We detected that such an alternating field provides an *easy* and in particular *accurate* controllable key parameter to trigger the system to change from subcritical to supercritical and vice versa. Main characteristics while "surfing the edge of instability" can be described as follows (schematics in Fig. 2): For small magnetic modulation amplitudes the system is supercritical for high frequencies Ω_H. Decreasing the frequency modifies this scenario and the system becomes temporally sub- and supercritical. On the other hand for large modulation amplitudes the system is subcritical in the high frequency limit.

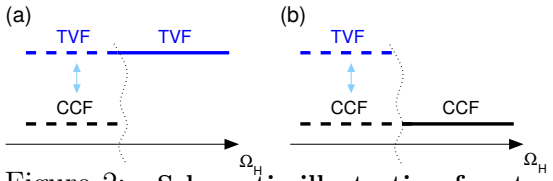

Figure 2: **Schematic illustration for stability change with Ω_H.** Schematic illustration the switch between sub- and supercritical flow states with variation in the driving frequency Ω_H (increasing left to right). (a) corresponds to scenario in Fig. 1.

Acknowledgments

S. A. is a Serra Húnter Fellow.

References

[1] S. Altmeyer, C. Hoffmann, A. Leschhorn, and M. Lücke, *Influence of homogeneous magnetic fields on the flow of a ferrofluid in the Taylor-Couette system.* Phys. Rev. E **82**, 016321 (2010).

[2] M. Niklas, *Influence of magnetic fields on Taylor vortex formation in magnetic fluids.* Z. Phys. B **68**, 493 (1987).

[3] S. Altmeyer, *On the ridge of instability in ferrofluidic Couette flow via alternating magnetic field.* Scientific Reports **11**, 4705 (2021).

[4] G. I. Taylor, *Stability of a viscous liquid contained between two rotating cylinders.* Philos. Trans. R. Soc. London A **223**, 289 (1923).

[5] M. Reindl and S. Odenbach, *Effect of axial and transverse magnetic fields on the flow behavior of ferrofluids featuring different levels of interparticle interaction.* Phys. Fluids **23**, 093102 (2011).

Alternating-current conductivity exhibited by magnetoactive elastomers with different fillers

A.V. Bakhtiiarov[1], G.V. Stepanov[1], D.A. Lobanov[1], D.A. Semerenko[2]

[1] *State Research Institute for Chemical Technologies of Organoelement Compounds, 111123, Shosse Entuziastov, 38, Moscow, Russia*
[2] *Bauman Moscow State Technical University, 105005, ul. Baumanskaya 2-ya, 5/1, Moscow, Russia*

One of the principal aspects of our studies of materials exhibiting the capability to vary their electrical conductivity under the influence of magnetic fields, also known as the magnetoresistive effect, is the search for appropriate compositions [1]. The goal of the present work is determination of the optimal formula as well as the conditions under which the functioning of the material would be most efficient. Having the means to fabricate silicone resin-based matrices with different elasticities, we focused our attention on problems connected to the specifics of filling. The investigations were carried out in areas related to the interior orientation and shapes of particles and their chemical composition.

Experiments dedicated to the investigations of the conductivity of the samples containing up to 82 wt.% of metal filling matter pointed to certain specific features of the system. In particular, even highly filled samples demonstrated extremely low direct-current conductivity which was a determining factor for doing the measurements using alternating current, which expanded the area of investigations. Indeed, every metal particle is a small piece of conducting material, and separated by a layer of isolator, every couple of them feature a non-zero capacitance. Therefore, the bulk of the composite may be considered as a set of a big number of capacitors, whereas the overall capacitive susceptance depends not only on the passing current frequency but also on the interior distribution of particles determined by an applied magnetic field. In addition, variation of filler composition by the introduction of nickel-electroplated carbonyl iron particles, which has the purpose to improve their conductive properties, it was noticed that their presence in the composite resulted in little change. For instance, the ratio of the resistivity determined at a field of 344 mT to that measured at zero-field at a frequency of passing current of 10 kHz was 20.9 for the sample containing 80 wt.% of untreated carbonyl iron particles (spherical shape), which was even better in comparison to a similar sample impregnated with nickel-electroplated particles (the decimal logarithms of the ratios are brought in the Table). The anisotropic sample filled with untreated iron particles showed a close result. A somewhat better output was given by the material prepared on the basis of plate-like particles produced from a carbonyl iron powder by milling in isopropanol with the following electroplating.

Table 1. Decimal logarithms (orders of magnitude) of the ratios of the resistivities at 344 mT to those at zero-field.

Filling	lg[ρ(344 mT)/ρ(0)] at 10 kHz
82 wt.% of Fe, spherical, 3-8 μm untreated isotropic anisotropic	 1.32 1.09
82 wt.% of Fe, spherical, 3-8 μm Ni-electroplated	1.07
82 wt.% of Fe, plate-like Ni-electroplated	1.66
72 wt.% of Fe, splinters, 3-8 μm untreated	2.55
72 wt.% of Fe, splinters, 3-8 μm Ni-electroplated	4.45

It is reasonable to assume that since the expected effects are evidently mitigated by the non-conducting silicone matrix, introduction of splinter particles might provide their closer approach under the influence of a magnetic field and by that be a solution. Measurements carried out on three samples containing particles obtained by milling a carbonyl iron powder in n-heptane indicated that the selected strategy was correct. The specimens highly filled with splinter particles indeed demonstrated an improved performance whereas the one containing nickel-electroplated particles showed the most promising result (Table 1).

With the purpose to compose a more complete picture of the conductive features of magnetoactive elastomers, the relationships between their resistivities and magnetic field strength were recorded at six frequencies in the interval 25 Hz – 1 MHz. As may be seen from the graphs presented (Figure 1), the material becomes more conductive as the frequency and magnetic field increase. Comparing the resistivity magnitudes at zero-field and at 344 mT, it may be noticed that the absolute magnetoresistive effect amounting for more than 6 orders of magnitude at 25 Hz for the sample with nickel-electroplated splinter particles decreases to a value of 3.5 at a frequency of 1 MHz.

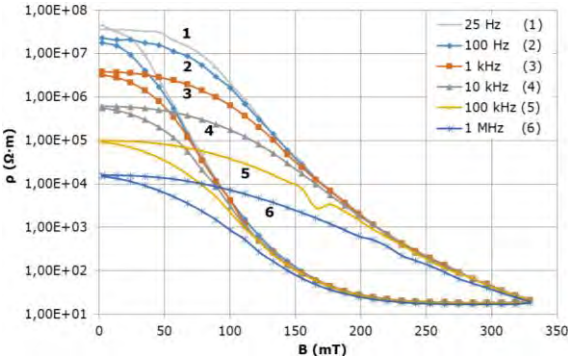

Figure 1. Dependence of the resistivity – magnetic field relationship on the frequency of passing current. Sample with Ni-electroplated splinter particles.

Whereas these results were obtained for isotropic samples, our future experimental work will be focused on materials with an interior preferred orientation as well.

Acknowledgments

This work is supported by the RFBR №19-53-12039.

References

[1] Stepanov G.V., Semerenko D.A., Bakhtiiarov A.V., and Storozhenko P.A. Magnetoresistive Effect in Magnetoactive Elastomers // J. Supercond. Nov. Magn. – 2013. – № 26. P. 1055–1059.

Field-controlled equilibrium shapes of a horizontal cantilever made of a magnetised magnetoactive elastomer

T. I. Becker[1], O. V. Stolbov[2], D. Yu. Borin[3], G. V. Stepanov[4], K. Zimmermann[1] and Yu. L. Raikher[2]

[1] *Technical Mechanics Group, Faculty of Mechanical Engineering, Technische Universität Ilmenau, 98684 Ilmenau, Germany*
[2] *Institute of Continuous Media Mechanics, Ural Branch of Russian Academy of Sciences, 614018 Perm, Russia*
[3] *Chair of Magnetofluiddynamics, Measurement and Automation Technology, Institute of Mechatronic Engineering, Technische Universität Dresden, 01062 Dresden, Germany*
[4] *State Scientific Research Institute of Chemistry and Technology of Organoelement Compounds, 111123 Moscow, Russia*

With a far-fetched objective to design a family of sensors using a cantilever of a magnetoactive elastomer (MAE) as a functional element, we consider theoretically and experimentally a horizontal cantilever made of a magnetised MAE filled with hard magnetic NdFeB particles. The MAEs of this type come out after preparation with a residual permanent magnetization (remanence) that makes them strongly controllable by externally applied fields of even small magnitudes. In our experimental set-up and in the arrangement that we use for modelling, the MAE remanence $\boldsymbol{M}$ is directed along the cantilever's length axis and thus normally to the gravity force $\boldsymbol{g}$, see Fig. 1.

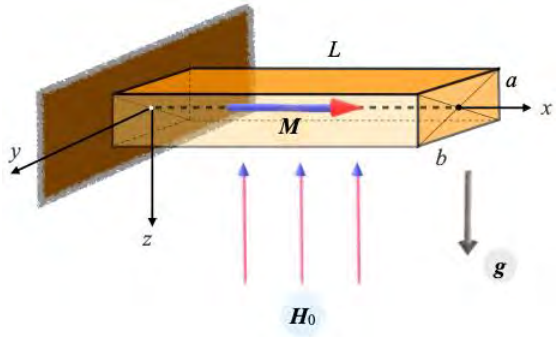

Fig. 1: MAE cantilever with a residual permanent magnetisation under the action of a uniform magnetic field and gravity.

Out of its magnetostatic preferences, the MAE cantilever would always tend to align its magnetic moment with the vertically applied uniform magnetic field $\boldsymbol{H_0}$. This tendency is enhanced by gravity in the case of a field directed downward and impaired in the opposite situation. Evidently, if the magnetic properties of an MAE were too weak, such a cantilever would never able to bend in the direction of the upward field.

Assuming realistic dimensional values (i.e. close to the experimental ones) of the cantilever's geometric, elastic and magnetic parameters, a finite-element modelling is performed that treats the problem as a coupled magnetoelastic one. The only simplification is that its formulation is made 2D, so that the plate in the scheme of Fig. 1 is infinite in the y direction. As it turned out in the *a posteriori* analysis, this assumption does not entail any qualitative changes in the cantilever deformations.

The experimental study is performed on a cantilever made of an MAE that is a two-component silicone rubber filled with spherical NdFeB particles of micron size (median diameter of 35-55 μm). The volume fraction of the hard ferromagnetic phase NdFeB is 10 %. The polymer matrix of the material is taken to be rigid enough. The Young modulus is estimated to be of the order of 10^7 Pa using the quasi-statically torsional tests. The mass density of the MAE is both measured and calculated as a linear combination of two substances of known mass densities: ρ = 1.66 g/cm^3. The polymerised cantilever is placed inside a powerful electromagnet and treated for a short time with a magnetic field of 0.8 T directed along the cantilever's length axis.

Comparison of the results of the MAE bending is presented in Fig. 2 for various

field strengths. The dashed lines mark the neutral axis of the cantilever obtained from the numerical modelling. In the experiment, one can register using a laser triangulation sensor only the contour of the upper or bottom surfaces of the cantilever. The measurements for the upper face are shown by dots. In Fig. 2, the data are presented in dimensional form, values of the applied uniform field are given in mT.

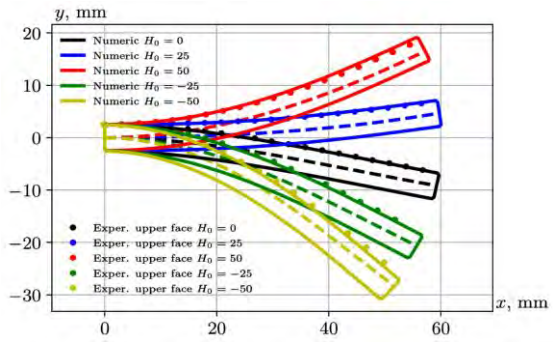

Fig. 2: Equilibrium shapes of the magnetised MAE cantilever for various field strengths: numerical (lines) and experimental (points) results.

As seen in Fig. 2, in the field-free configuration (black colour), the cantilever dwells with a pronounced downward bend and readily enhances it under a downward (denoted as negative) field. Under a positive, i.e. upward, field, the cantilever is well able to overcome the gravity and to bend upward.

In conclusion, according to the obtained results, the 2D model yields quite reliable quantitative estimates, being as well more convenient to use in comparison with a 3D one. The experiment has proven that an MAE cantilever that is a few centimeters long and a few millimeters thick is able to respond to a field of quite moderate strength with a rather large spatial deflection. However, it should be remarked that as the experiment reveals, the considered configuration of the MAE cantilever incorporates a feature that might to some extent spoil the accuracy of measurements. This is a consequence of viscoelasticity of the material, most probably due to the nature of its matrix. The retarded mechanical reaction entailed by an extremely wide spectrum of relaxation times – the feature that is ubiquitous in elastomers – results in particular in the so-called "training effect" that should be taken into account. Certainly, when choosing an MAE material for a cantilever-like functional element, one has to choose between softer matrixes, which show a larger response deflection, but enhanced retardation effect, and stiffer ones that demonstrate a reduced deflection, but provide greater reproducibility.

Acknowledgments

This work is supported by the Deutsche Forschungsgemeinschaft (DFG) and the Russian Foundation for Basic Research (RFBR) through SPP1681 and PAK907 under the projects BE 6553/2-1, ZI 540-17/3, BO 3343/3-1, 19-53-12039 and 19-52-12045.

References

[1] Becker T.I., Stolbov O.V., Borin D.Yu., Zimmermann K. and Raikher Yu.L. Basic magnetic properties of magnetoactive elastomers of mixed content. Smart Mater. Struct. 29 (2020) 075034.

Shape-induced superstructure formation in concentrated ferrofluids

P. Bender[1], R. P. Hermann[2,3], S. Disch[4,*]

[1]*Heinz Maier-Leibnitz Zentrum (MLZ), Technische Universität München, Germany*
[2]*JCNS-2, PGI-4, Forschungszentrum Jülich, Germany*
[3]*Materials Science and Technology Division, Oak Ridge National Laboratory, United States*
[4]*Department für Chemie, Universität zu Köln, Germany*

The response of magnetic nanoparticles (MNPs) to applied static and dynamic magnetic fields is the subject of intense research in view of its fundamental technological importance, *e.g.*, for medical applications such as imaging and magnetic hyperthermia [1], or sensor applications [2]. The field-assisted self-organization of shape-anisotropic nanoparticles in dispersions is further desired for liquid crystalline or optically anisotropic materials [3] and as a prerequisite for self-organization into long range ordered arrangements [4]. The heating behavior of MNPs in AC magnetic field is largely influenced by interactions arising from nanoparticle aggregation [5]. A detailed understanding of interparticle interactions in colloidal dispersion is therefore crucial for the advancement of magnetic hyperthermia.
A variety of nanoparticle arrangements has been observed for colloidal dispersions of spherical MNPs with different particle sizes, ranging from reversible chain-formation [6] to extended columns [7], or even crystalline arrangements of MNPs [8]. The strong structure-directing influence of the particle shape on the symmetry of mesocrystalline arrangements has been studied in detail for nanocubes with a varying degree of corner truncation [9–11]. In this contribution, we present the influence of the particle shape on the superstructure formation in concentrated colloidal dispersions.

The nanoparticles under study consist of maghemite (γ-Fe_2O_3) nanospheres and nanocubes

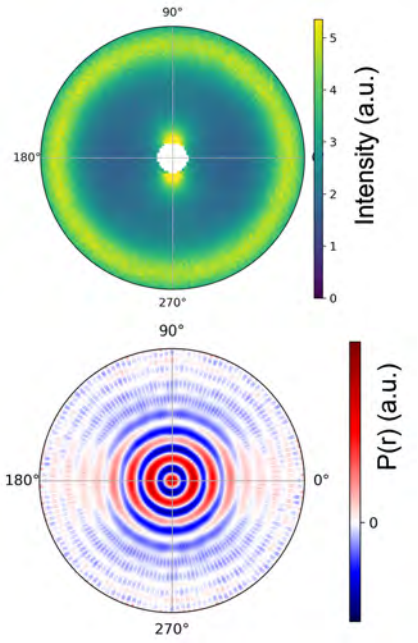

Figure 1: a) SANS pattern of nanocubes in a 1.5 T magnetic field (applied horizontally) b) 2D pair distance distribution derived by SVD.

with a 9 nm diameter and 8.5 nm edge length, respectively, and excellent monodispersity with lognormal size distributions of 5.5(1) % and 7.2(2) % FWHM. The integral nanoparticle moment of the samples is very similar, with a stronger degree of surface-near spin disorder in the nanocubes [12]. Despite the similar particle size, magnetic moment, and volume concentration (>5 vol-%), we observe a significantly distinct aggregation behavior of nanospheres and nanocubes using Small-Angle Neutron Scattering (SANS).

Both samples reveal a short range ordered hard spheres interaction potential with random orientation towards an applied magnetic field that is observed as ring-shaped correlation peak in the 2D SANS detector (Fig. 1a). The particle-particle distances derived from the peak position are significantly smaller than observed in ordered assemblies of the same particles [9, 10], and a preference of face-to-face orientation of the nanocubes is likely. The distinct aggregation behavior of the cubic nano-particles is expressed in a much stronger correlation peak which exhibits an unusual field-dependence suggesting field-induced order and structural rearrangement. Additionally, a directionally anisotropic scattering contribution observed in the lower Q range indicates oriented attractive interparticle interactions of the nanocubes. This becomes visible in the 2D pair distance distribution function extracted from the 2D scattering pattern using the Singular Value Decomposition approach (Fig. 1b) [13], which we interpret as an internally nearly isotropic superstructure which extends anisotropically in the field direction.

In our contribution, we give a detailed account on the impact of nanoparticle shape on the *inter*particle correlations in colloidal dispersions of maghemite nanoparticles. Particular emphasis is on the aggregation behavior of cubic particles in highly concentrated dispersions. Geometric orientation and agglomeration of the particles will be discussed as suggested by field-dependent SANS experiments.

Acknowledgments

We acknowledge the provision of beam time at the instrument D22 at the Institut Laue-Langevin, Grenoble, France. Albrecht Wiedenmann is acknowledged for his support in data acquisition at D22.

References

[1] Q. A. Pankhurst *et al.*, *J. Phys. D: Appl. Phys.* **36**, R167 (2003).

[2] D. T. N. Chen *et al.*, *Annual Review of Condensed Matter Physics* **1**, 301 (2010).

[3] G. M. Whitesides, B. Grzybowski, *Science* **295**, 2418 (2002).

[4] A. Ahniyaz *et al.*, *Proc. Natl. Acad. Sci. U.S.A.* **104**, 17570 (2007).

[5] I. Andreu, A. Urtizberea, E. Natividad, *Nanoscale* **12**, 572 (2020).

[6] N. Nandakumaran *et al.*, *Adv. Mater.* **33**, 2008683 (2021).

[7] M. Klokkenburg *et al.*, *Phys. Rev. E* **75**, 051408 (2007).

[8] Z. Fu *et al.*, *Nanoscale* **8**, 18541 (2016).

[9] S. Disch, E. Wetterskog *et al.*, *Nano Letters* **11**, 1651 (2011).

[10] S. Disch *et al.*, *Nanoscale* **5**, 3969 (2013).

[11] E. Wetterskog *et al.*, *Nanoscale* **8**, 15571 (2016).

[12] S. Disch *et al.*, *New J. Phys.* **14**, 013025 (2013).

[13] P. Bender *et al.*, *Acta Cryst. A* **75**, 766 (2019).

Development of a soft gripper end-effector based on magnetorheological elastomers

J. Chavez[1,2], T. Kaufhold[1], V. Böhm[2], K. Zimmermann[1]

[1] *Technische Universität Ilmenau, Department of Mechanical Engineering, Technical Mechanics Group*
[2] *Ostbayerische Technische Hochschule Regensburg, Department of Mechanical Engineering*

Introduction

This work shows the investigations on magnetorheological elastomers containing soft magnetic particles, with the focus on their potential application as end-effectors for soft gripping technology. After numerous experimental investigations, a suitable material composition and geometry is found for a soft end-effector with enhanced performance. Theoretical investigations were carried out to quantify on the macroscale the magnetic and mechanical properties of the materials in use. Additionally, a procedure is developed to enable the description of their magneto-mechanical behaviours by using the finite element method. The research is concluded in a real prototype which shows the execution of the end-effector, its magnetic activation and demonstrates the applicability for manipulation purposes.

Theoretical approaches

Investigations with cylindrical samples of magnetorheological elastomers (MREs) made of carbonyl iron powder (CIP) were performed to observe the magnetic attractive force to a cylindrical permanent magnet. In the analysis, an expression was determined for this magnetic force. The force depended on the relative permeability μ_{MRE} of the MRE sample and geometrical parameters. In turns, μ_{MRE} depends on the volume fraction φ of the CIP in the sample. In this regard, the μ_{MRE} value of the MRE samples exhibits an exponential relation of the relative permeability of pure CIP particles, μ_{CIP}, and φ, as follows [1]:

$$\mu_{MRE} = (\mu_{CIP})^{\varphi} \qquad (1)$$

Magneto deformation analysis

For the applicability of MRE in soft grippers' end-effectors, two main properties are to be considered when magnetic fields are applied: field-stiffening [2] and field-induced plasticity [3]. The first refers to the stiffening of the MRE due to the re-accommodation of the particles, following the magnetic field lines. The second to the shape recorded on the material when deformed by objects while a magnetic field is applied. In real applications, these effects occur simultaneously, meaning that during the deformation by the object to be gripped, the MRE can at the same time become stiffer.

The significance of these effects depends fundamentally on the material composition of the MRE and the magnitude of the applied magnetic field. Furthermore, the influence of both effects to each other is also related to the geometry of the MRE-based end-effector. Thus, the analysis for simultaneous field-stiffening and field-induced plasticity outcomes complex to be detailed for a general MRE volume. In this context, discs of MRE samples were fabricated with a specific composition (30 vol.% CIP, 31.5 vol% silicone oil, elastomer matrix: Neukasil RTV 26 + catalyzer A7). The MRE discs were encapsulated at their lateral sides, permitting a deformation of the central area due to the magnetic attraction to a permanent magnet placed in the vicinity. These areas had an effective deformable radius of 8…32 mm.

The mechanical behaviour of the MRE is modelled with the Mooney-Rivlin model of 3 parameters for hyperelastic materials and the magneto-deformations of the discs are

computed through the use of the finite element method (FEM) in iterative steps [4]. At each iterative step, a finite element has a certain set of the 3 parameters which depends on its averaged magnetic flux density (B_i) and an attractive force towards the permanent magnet is calculated. The magneto-deformation with the successive iterations results in a modification of the mechanical properties and the magnetic attraction to the magnet (Fig. 1). The increment of attractive force is applied in the subsequent iterations until no perceptible additional magneto-deformation is recognised. The simulated results approached with great accuracy the experimental ones.

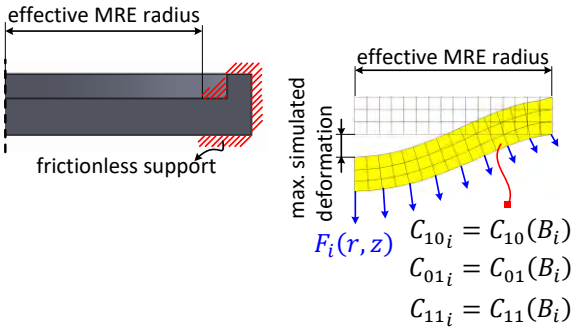

Figure 1. Iterative magneto-deformation computed by the use of FEM.

MRE-based end-effector prototype

The expertise in the design of magnetically end-effectors for gripping purposes exhibited that a hollow rotational body is of much advantage for the sought application [5]. The exemplarily prototype consist of a main MRE membrane which enables the shape adaptation, a non-magnetic hard elastomer which serves as support and highly elastic chambers attached to enhance the shape adaptation by relieving the inner pressure during the deformation.

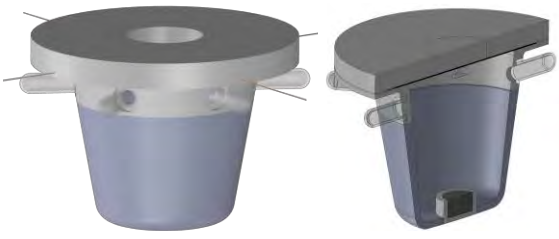

Figure 2. Outline for the MRE-based end-effector prototype: end view (left) and section view (right).

Additionally, the prototype contains a layer of elastomer with embedded carbon black powder (CBP) to enable sensory functionality [6]. By detecting a change in the electrical resistance of this layer, the maximum permitted deformation is recognised and thus, the shape adaptation procedure stopped.

Acknowledgments

This work was supported by Deutsche Forschungsgemeinschaft (DFG), project ZI540-17/3 within the priority program SPP1681.

References

[1] J. Chavez et al.: "A method to approach constant isotropic permeabilities and demagnetization factors of magneto-rheological elastomers", in: J. of Magnetism and Magnetic Materials, 2021, vol. 527, 167742, 10 p.

[2] Y. Han et al.: "Field-stiffening effect of magneto-rheological elastomers", in: Int. J. of Solids and Structures, 2013, vol. 50, nr. 14-15, pp. 2281-2288.

[3] P. Melenev et al.: "Modeling of the Field-Induced Plasticity of Soft Magnetic Elastomers", in: J. of Intelligent Material Systems and Structures, 2011, vol. 22, nr. 6, pp. 531-538.

[4] K. Zimmermann et al.: "Theoretical and experimental investigations of magnetic hybrid materials with applications for locomotion, manipulation and sensor systems in soft robotics", in: *Accepted publication: Monkman G., Soft robotics*.

[5] J. Chavez Vega et al.: "Towards Magneto-Sensitive Elastomers based End-effectors for Gripping Application Technologies", in: Proc. of IEEE International Conference on Mechatronics (ICM), 2019, pp. 217-222.

[6] N. Prem et al.: "Properties of Polydimethylsiloxane and Magnetoactive Polymers with Electroconductive Particles", in: Macr. Chem. and Phys., 2018, vol. 219, nr. 18, 1800222, 8 p.

Comparison of a practical and a theoretical approach to determine the bending curves of magnetic alginate hydrogel strings depending on particle concentration and aging

C. Czichy[1], S. Odenbach[1]

[1] *Chair of Magnetofluiddynamics, Measuring and Automation Technology, TU Dresden, 01069 Dresden, Germany*

Introduction

A goal in Tissue Engineering is to create patient specific implants through additive manufacturing to replace defect or destroyed tissue and restore its function. Therefore, scaffolds are generated, which are colonized with stem cells [1]. These cells can be animated e.g. through mechanical stimuli to differentiate and / or to multiply. A new approach for deforming the scaffolds is to apply an alternating magnetic field to a magnetic hydrogel [2]. The characterization of the deformation is described in this work.

Materials

The main component of the matrix was a hydrogel of 3 wt% alginate, which was dissolved in phosphate buffered saline (PBS). Aiming to make it suitable for extrusion printing methylcellulose (9 wt%) as gelling agent was added. As magnetic particles magnetite microparticles were chosen. The concentrations were 5, 15, 25 and 35 wt%.
The samples were stored in cell culture medium for 14 days at 37 °C. The medium was renewed two times per week.

Theoretical approach

In an attempt to characterize this particle-matrix-system a simple and well-known geometry for a cylinder was chosen with a bending beam setup. The bending curve, w, depends on the coordinate in longitudinal direction of the sample, y:

$$w(y) = \frac{q\,l^4}{24\,E\,I_x}\left(\frac{y}{l} - \frac{2\,y^3}{l^3} + \frac{y^4}{l^4}\right) \qquad (1)$$

Thereby I_x is the moment of inertia, E is the Young's modulus, detailed descriptions are found at Czichy et al. [3], and q is a linear load over the whole length l of the sample with q(y) = F l = constant.
The deforming force corresponds to the Kelvin force, which by the chosen setup and the assumptions of a homogeneous magnetization simplifies to:

$$\vec{F} = \mu_0\, V\, M_V\, \nabla\vec{H} \qquad (2)$$

with the magnetic permeability of the vacuum μ_0, the volume V, the volume magnetisation M_V and the magnetic field gradient $\nabla\vec{H}$. The field was designed for an elongation of 10 % at day 14.
The geometric parameters are defined by the manufacturing process and were measured for each sample via the micro-computer tomography (µCT). The magnetisation was measured with a VSM.
Taking the error tolerance into account, an upper and a lower boundary were determined for the different samples. Instead of a mean value these boundaries were used for the comparison.

Practical approach

To determine the actual deformation an experimental setup for the µCT was build. Using a Maxwell-setup a constant magnetic field gradient could be applied.
Before applying the magnetic field, a µCT scan was taken in order to create a 3D image of the initial situation. From this data the neutral fiber $z_i(y)$ could be determined with z as the coordinate in field direction. Subsequently, the field was applied and a second scan was taken from the new situation, resulting in the neutral fiber with $z_{MF}(y)$. The

difference $z_i - z_{MF}$ corresponds to the bending curve w.

Results and Conclusion

These experiments were performed for different particle concentrations on day 0 after crosslinking, on day 1 and on day 14.
Fig. 1 shows the measured bending curve for a sample on day 14 with 25 wt % magnetite. It can be seen that the measured bending curve lies between the upper and the lower boundaries of the calculated bending curve.

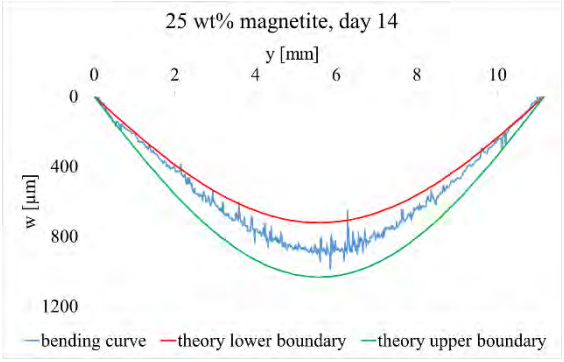

Figure 1. Measured bending curve of an alginate-methylcellulose-sample with 25 wt% magnetite compared to the upper and lower boundary of the calculated bending curve.

For all of the particle concentration and measuring points this could be observed. From this it can be concluded, that the presented theoretical method is suitable to predict the deformation behavior. Which results in the verification that a complex structure as a scaffold can be simulated with a qualified program. Also, for new developments it is sufficient to measure the Young's moduli and the magnetization without the experiments regarding the bending curves.

Acknowledgments

The authors would like to thank the European Social Fund (ESF) and the Free State of Saxony for financial support of this project in the course of the ESF Young Researchers Group IndivImp at TU Dresden.

References

[1] Schütz, Placht, Paul, Brüggemeier, Gelinsky, Lode: „Three-dimensional plotting of a cell-laden alginate/methylcellulose blend: towards biofabrication of tissue engineering constructs with clinically relevant dimensions“ journal of tissue engegineering and regenerative medicine 11, p1574-1587, 2017, John Wiley & Sons, Ltd., doi:10.1002/term.2058

[2] Spangenberg, Kilian, Czichy, Ahlfeld, Lode, Günther, Odenbach, Gelinsky: Bioprinting of Magnetically Deformable Scaffolds", ACS Biomater. Sci. Eng 2, p648-662, 2021, https://dx.doi.org/10.1021/acsbiomaterials.0c01371

[3] Czichy; Spangenberg; Günther, Gelinsky, Odenbach: "Determination of the Young's modulus for alginate-based hydrogel with magnetite-particles depending on storage conditions and particle concentration" Journal of Magnetism and Magnetic Materials 2020, 501, 166395

Hybrid nanomaterials of biomolecule corona coated magnetic nanoparticles and their interaction with biological systems

S. Dutz[1,2], A. Weidner[1], M. v.d. Lühe[3,4], C. Gräfe[5], P. Biehl[3,4], J. Demut[5], P. Warncke[6], S. Jungmann[6], D. Fischer[4,6,7], F.H. Schacher[3,4], J.H. Clement[4,5]

[1] *Institute of Biomedical Engineering and Informatics (BMTI), Technische Universität Ilmenau*
[2] *Department of Nano Biophotonics, Leibniz Institute of Photonic Technology (IPHT), Jena*
[3] *Institute of Organic Chemistry and Macromolecular Chemistry (IOMC), Friedrich-Schiller-University Jena*
[4] *Jena Center for Soft Matter (JCSM), Friedrich-Schiller-University Jena*
[5] *Klinik für Innere Medizin II, Abteilung Hämatologie und Internistische Onkologie, Universitätsklinikum Jena*
[6] *Institute of Pharmacy, Pharmaceutical Technology und Biopharmacy, Friedrich-Schiller-University Jena*
[7] *Department for Chemistry and Pharmacy, Chair of Pharmaceutical Technology, Friedrich-Alexander-Universität Erlangen-Nürnberg*

Introduction

One of the main obstacles for the medical use of magnetic nanoparticles (MNP) is their behavior when applied to biological liquids and biological systems, like the human body. For decades chemists, biologists, and engineers have developed methods to stabilize the MNP in aqueous suspensions and test biocompatibility *in vitro* and *in vivo*. After application of MNP into a biological system, it was found that the MNP are immediately covered by biomolecules available within the biological system. A so-called "biomolecule corona" is formed that changes the behavior of the MNP drastically and gives them a new biological identity. This biomolecule coating, consisting mainly of proteins and lipids, directly influences the properties of the used MNP. The biomolecule corona alters surface chemistry and thus their stability against agglomeration and sedimentation as well as their interaction with biological systems *in vitro* and *in vivo*. The knowledge of the influencing factors on an evolving biomolecule corona and the possibilities to control and to include the corona formation as a favorable event for further applications is of major importance for the preparation of biocompatible MNP suspensions.

Methods

Aim of our work has been to develop procedures for the preparation of biocompatible suspensions of biomolecule coated MNP. Main approach to achieve this objective was the pre-incubation of the MNP in a biological fluid like FBS, serving as a source for the formation of the biomolecule corona under controlled conditions to investigate the evolving biomolecule corona and to study the interactions of the magnetic nanohybrids with biological systems *in vitro* and *in vivo*. For this, we investigated and optimized MNP systems with different cores and different coatings featuring varying surface charges and charge patterns (positive, negative, neutral, zwitterionic). We tested the influence of these parameters together with the parameters for the pre-incubation procedure (e.g. temperature and time) on the resulting structure and amount of biomolecules bound to the surface of the MNP. Additionally, we investigated the interactions of these magnetic nanohybrids with biological systems like cells as well as *in vivo* assays using the shell-less hen's egg test on the chick area vasculosa (HET-CAV). Furthermore, we developed strategies to sterilize and store the magnetic nanohybrids for long term, which is crucial towards medical applications.

Results

Our investigations reveal that within seconds after bringing MNP in contact with a biological fluid, a biomolecule corona is formed on the surface of the particles.

For the most of the here tested core/shell MNP, our TGA results show that at lower temperatures (25 and 37 °C) the amount of biomolecules does not rise with increasing incubation time whereas this is the case at elevated temperatures (50 and 70 °C). The amount of biomolecules adsorbed to the surface of the core/shell MNP can be tuned by the composition of the incubation media. A higher amount of biomolecules in the incubation media increases the volume of the biomolecule corona and results in a larger thickness of the biomolecule coating.

A semi-quantitative analysis of corona composition derived from SDS-PAGE confirmed for all coating materials and temperatures an influence of those on the ratios between low molecular weight proteins (<25 kDa), medium molecular weight proteins (25 - 100 kDa), and high molecular weight (>100 kDa) proteins, but no general trends can be derived from the obtained data so far.

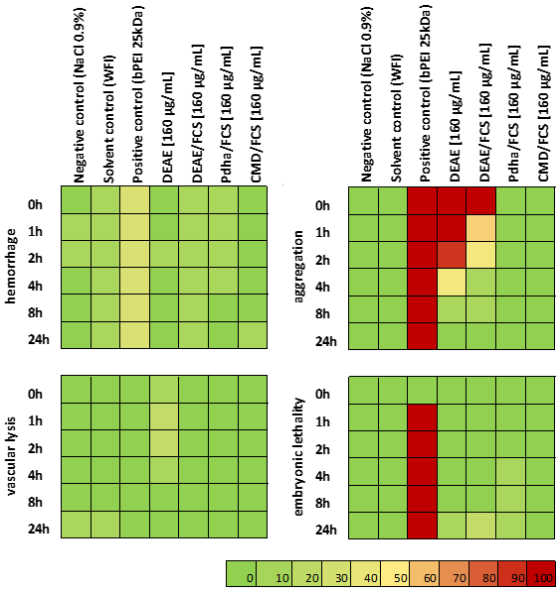

***Figure 1**: Probability for the occurrence of adverse effects for different particles and time points within the shell-less hen's egg model serving as a test to evaluate the in vivo toxicity of the magnetic nanohybrids (% positive control).*

In cell viability tests no cytotoxicity was observed for all tested biomolecule coated MNP. A higher amount of biomolecules adsorbed to the surface foster cell viability. Laser scanning microscopy revealed that a more pronounced biomolecule corona retarded the uptake of MNPs into the cells. We could demonstrate that the cellular uptake and adhesion processes can be controlled by the extent of a biomolecule coating on the magnetic nanohybrids.

By using a shell-less hen's egg model, no adverse effects of all biomolecule coated MNP for this *in-vivo*/*ex-ovo* test were determined, except DEAE that serves as a test to increase biocompatibility of a toxic coating (see figure 1). Resulting from these investigations, we were able to show that the *in vivo* biocompatibility of our newly developed nanohybrids under the applied conditions could be highly improved by the biomolecule coating.

For the sterilization by means of UV radiation, we found a perfect sterilization but no damaging effects for biomolecule coated MNP. Contrary, the treatment of biomolecule coated particles by means of autoclaving leads to significant changes in the integrity of the proteins and thus this method is not suitable for sterilization. During lyophilization, the addition of PEG to the samples revealed well-dispersed fluids after re-suspension of the powders.

Conclusion

We developed and described a novel type of hybrid nanoparticles with improved biocompatibility for medical application. These magnetic nanohybrids bear a second coating of biomolecules, which enables the control of the interaction of these particles with biological systems. The biomolecule corona may mask adverse effects on biological systems of cytotoxic MNP.

Acknowledgments

This work was supported by the Deutsche Forschungsgemeinschaft (DFG) in the framework of SPP 1681 (FKZ: CL202/3-1, CL202/3-2, CL202/3-3, DU1293/4-1, DU 1293/4-2, DU1293/7-3, and SCHA1640/7-1). The authors thank all partners within the SPP 1681 for the fruitful and pleasant collaboration.

Evaluation of the determination of the core-shell structure of MNP and its opsonisation layer

D. Eberbeck[1], M. Kruteva[2], L. Fruhner[2], A. Feoktystov[3], R. Thiermann[4], A. Tschöpe[5], F. Wiekhorst[1]

[1] *Physikalisch-Technische Bundesanstalt, Berlin, Germany*
[2] *Forschungszentrum Jülich GmbH, JCNS-1 & IBI-8, 52425 Jülich, Germany*
[3] *Forschungszentrum Jülich GmbH, Jülich Centre for Neutron Science JCNS at Heinz Maier-Leibnitz Zentrum MLZ, 85748 Garching, Germany*
[4] *Fraunhofer-Institut für Mikrotechnik und Mikrosysteme IMM, Mainz, Germany*
[5] *University of Saarland, Department of Experimental Physics, Saarbrücken, Germany*

The opsonisation of magnetic nanoparticles (MNP) in an organism crucially determines their effect and fate after administration. For example, nanoparticles opsonised by the abundance of clustering proteins show a reduced cellular uptake (stealth effect) [1]. Furthermore, type and quality of MNP coating crucially determine the opsonisation. For example, the half-life period of MNP receiving a second PEGylation during synthesis could be enhanced from minutes to about 1 hour [2].

Hence, the choice of the right MNP system for a biological application requires the selection of a proper coating. Their in-vitro opsonisation behaviour can be determined by in-vitro experiments.

Here, we determined the thickness and the density of the non-magnetic shell of the MNP together with the thickness of the opsonisation layer (here bovine serum albumin (BSA)). We used two single-core-shell MNP systems (SHP-30, Ocean Nanotech, USA) which are appreciated due of their well-defined spherical core-shell-structure and narrow core size distribution. These two systems differ strongly in its magnetisation behaviour. Established techniques to determine the thickness of the coating and opsonisation layer are measurements of the hydrodynamic diameter and core diameter as well as differences of the MNP diameters with and without opsonisation layer.

Is the accuracy of these methods sufficient to cope with deviations from ideal structure?

For a comprehensive characterisation of the physical and magnetic structure, the MNP were measured with Transmission Electron Microscopy (TEM), Small Angle X-ray and Neutron Scattering (SAXS, SANS), quasistatic field dependent magnetisation (M(H)) and alternating current susceptibility (ACS). Then a model that links the physical core-shell-structure of size distributed cores with its magnetic structure was fitted to all data sets, simultaneously. The magnetic structure was phenomenologically ascribed to a multi domain structure, comprising a leading domain linked to the core size and size distributed smaller domains (Fig. 1) with the volume fraction ϕ_{m2}. These smaller domains may represent, for example, weak magnetic areas (WMA) which may include the so called magnetic dead layer or other magnetically weaker phases like for example wustite that was found in SHP particles.

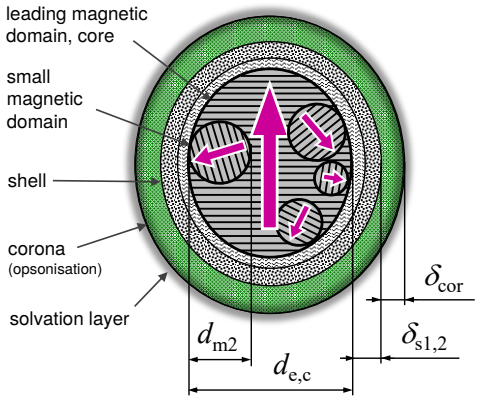

Figure 1: Core-shell model of a MNP with an ellipsoidal multi domain core, a double shell, and a corona.

Beyond the WMA, the "full" model also comprises aggregates of MNP, phenomenologically described as a fraction of larger particles. Additionally, a "simple" model

was applied using size distributed spherical core-shell particles, only.
While the "full" model describes the data quite well, the "simple" model does not (Fig. 2). Specifically, the clusters are attributed to cause the steeper increasing SAXS intensities towards $q = 0$ (Fig. 2a) as well as to the better describe the ACS-data, the WMA to the absence of saturation behaviour in M(H) (Fig. 2c) and the observed absolute values of ACS-data.

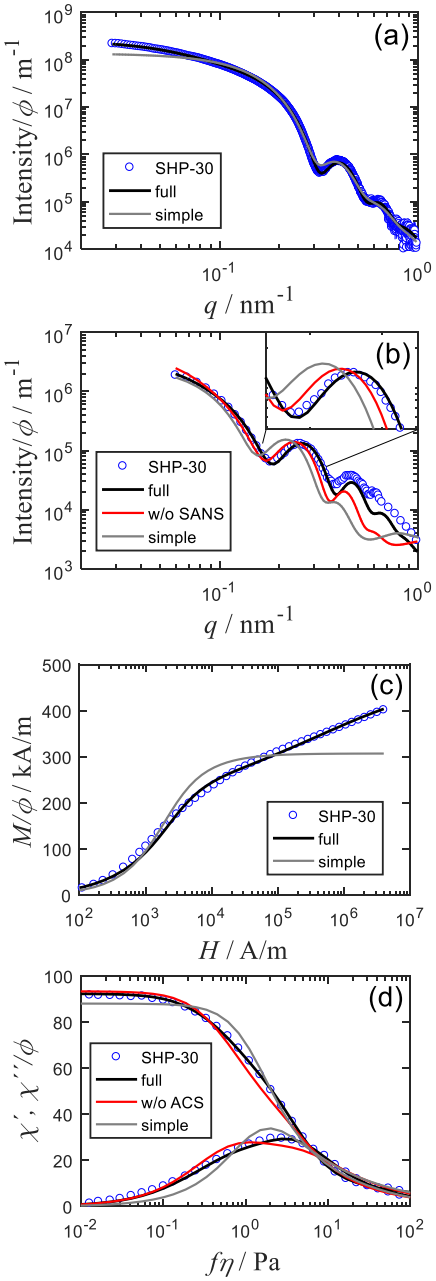

Figure 2. Simultaneous fit of the "simple" and "full" MSM to (a) SAXS, (b) SANS (MNP in D_2O→shell specific signal), (c) M(H) and (d) ACS data. As an alternative, data sets ACS or SANS were disregarded while fitting ("w/o ACS", "w/o SANS").

Is it possible to get good estimates of the coating and the opsonisation layer without harnessing hardly available SANS?

The full model was fitted omitting SANS or ACS data. Then the model curves for these data were calculated applying these parameters, now fitting exclusively the method specific parameters (Fig. 2b,d, "w/o…"). The deviations from the data are significant and attest a residual mismatch of the model to describe the real structure. This is also seen by the still significant deviations of the full model from the M(H) data at small fields (Fig. 2c). Accordingly, the omission of the SANS data leads to a change of the obtained value of the parameter of the thickness of the second MNP shell, δ_{s2}, from 3.7(1) nm to 5.7(4) nm for SHP-30 and from 4.1(3) nm to 0(1) nm for SHP-30B, respectively. The thicknesses of the corona, δ_{cor}, did not changed, because of the existence of the exact ACS reference data for the sample with opsonisated MNP. For SHP-30B, the fitted model deviates more from SANS data than it does for SHP-30. A deviation of the coating structure from a homogeneous shell will be discussed. Probably, this is linked to the higher value of $\delta_{cor} = 6.5(6)$ nm and lower value of its density, $\phi_{cor} = 0.06(1)$ nm, in comparison to $\delta_{cor} = 1.5(3)$ nm and $\phi_{cor} = 0.3(1)$ nm, respectively, obtained for SHP-30.

Conclusion: While the thickness of the opsonisation layer can be determined from ACS data alone, contrast variation of small angle scattering is necessary for a robust estimation of the coating thickness. By multimodal data analysis the core structure could reasonably linked to the MNP's magnetic behaviour.

Acknowledgments

This work was supported by the DFG priority program 1681.

References

[1] S. Schöttler et. al., Nat. Nanotechnol. 2016 114 **11**, 372 (2016)

[2] H. Kratz et. al., Nanomat. **9**, 10 (2019)

Magnetostriction of magnetic gels and elastomers – overall deformation based on a particle-resolved mesoscale description

L. Fischer, A. M. Menzel

Institut für Physik, Otto-von-Guericke-Universität Magdeburg, Universitätsplatz 2, 39106 Magdeburg, Germany

Introduction. – Magnetic gels and elastomers consist of magnetic or magnetizable colloidal particles enclosed by a soft elastic polymeric matrix [1, 2]. When they are exposed to homogeneous magnetic fields, two main effects arise [1–4]. On the one hand, the materials typically change their overall mechanical stiffness, which is referred to as magnetorheological effect. On the other hand, they may show reversible overall deformations, which is termed magnetostriction. While we have focused on the first effect in several previous studies [5–7], we now turn to the second one.

Scope. – Our goal is to describe these effects theoretically while we establish possible avenues for tailoring the magnetostrictive response. We explicitly aim at calculating analytically the overall deformation, and we start from the presence of individual magnetizable particles in the elastic matrix. To achieve this challenging goal, we consider the simplest geometries, which are spherical in shape. In fact, as we demonstrate, it is possible to derive analytical formulae for the displacement field for such objects within linear elasticity theory, assuming a homogeneous and isotropic elastic material [8]. In the literature, experimental example systems for comparison feature randomly distributed particles inside the elastic matrix. Such samples were observed to elongate along an external magnetic field direction [9].

Theoretical approach. – To make progress, we consider identical particles that are magnetized to saturation when the external field is switched on. Magnetic interactions are described using magnetic dipoles. This simplified approach is justified when the distance between the particles is large enough. The mutual magnetic forces between the particles lead to their displacements against the surrounding elastic material. Resulting elastic interactions between the particles through the elastic medium can be calculated to a given order [10–13]. These effects that we previously considered in an infinitely extended medium are now evaluated in finite-sized spheres. The consequences on the overall deformation of the spheres are determined [8].

Comparison with experiments and predictions. – In this way, we reproduce the experimental result for random internal particle distributions under the mentioned assumptions [8, 9]. Along these lines, we further address additional, prescribed particle arrangements. We concentrate on the magnetically induced change in volume and the relative elongation or contraction along the external magnetic field direction. Our explicit calculations quantify the corresponding response, that is, the relative elongation or contraction of the sphere along the applied external magnetic field. The result crucially depends on the particle configuration. Simultaneously, we evaluate the consequence that the matrix compressibility has on the type of observed deformation [8].

Twist actuators. – One special type of particle arrangement within the elastic matrix corresponds to twisted configurations. We here distinguish between two struc-

tures: globally twisted ones and individually twisted helices placed side by side. Our results suggest that both can lead to an overall twisting deformation of the elastic material [14]. Out of these two, the globally twisted structures show a purer twist-type deformation. Accordingly, through homogeneous external magnetic fields, a torsional actuator can be realized, which might be beneficial, for instance, for microfluidic mixing applications. In this context, we further connect a basic analytical mesoscopic model to a macroscopic continuum description [15]. To this end, we explicitly calculate some of the macroscopic material parameters as analytical expressions of the mesoscopic system parameters.

Size distribution. – Another aspect to address when comparing calculations to experimental realizations is the polydispersity of the magnetizable particles. We modify our description to allow for a simple study of the effects that different particle sizes introduce. For simplicity, we here use a binary size distribution to facilitate a systematic investigation. The studies are performed by keeping each spatial configuration of the sites of magnetizable particles fixed while changing their size. We find that an adjusted placement of larger and smaller particles can lead to qualitatively different types of deformation.

Conclusions. – Together, our investigations demonstrate how mesoscopic arrangements of discrete particles can affect the overall magnetostrictive response of magnetic gels and elastomers. This is important for their use as soft actuators or artificial muscles. We hope that our work will stimulate further experimental investigations and development of techniques that allow for prescribed placement of magnetizable inclusions in soft elastic environments.

Acknowledgments

We thank Stefan Odenbach and his team for their effort in establishing the SPP 1681 and fostering continuous interactions within this community. Support by the German Research Foundation (DFG) through the SPP 1681 over the past few years and a Heisenberg Grant is gratefully acknowledged.

References

[1] S. Odenbach, Arch. Appl. Mech. **86**, 269 (2016).

[2] R. Weeber, M. Hermes, A. M. Schmidt, C. Holm, J. Phys.: Condens. Matter **30**, 063002 (2018).

[3] A. M. Menzel, Arch. Appl. Mech. **89**, 17 (2019).

[4] A. M. Menzel, H. Löwen, Phys. Sci. Rev. DOI: 10.1515/psr-2019-0088.

[5] P. Cremer, M. Heinen, A. M. Menzel, H. Löwen, J. Phys.: Condens. Matter **29**, 275102 (2017).

[6] G. Pessot, M. Schümann, T. Gundermann, S. Odenbach, H. Löwen, A. M. Menzel, J. Phys.: Condens. Matter **30**, 125101 (2018).

[7] S. Goh, R. Wittmann, A. M. Menzel, H. Löwen, Phys. Rev. E **100**, 012605 (2019).

[8] L. Fischer, A. M. Menzel, J. Chem. Phys. **151**, 114906 (2019).

[9] C. Gollwitzer, A. Turanov, M. Krekhova, G. Lattermann, I. Rehberg, R. Richter, J. Chem. Phys. **128**, 164709 (2008).

[10] M. Puljiz, S. Huang, G. K. Auernhammer, A. M. Menzel, Phys. Rev. Lett. **117**, 238003 (2016).

[11] M. Puljiz, A. M. Menzel, Phys. Rev. E **95**, 053002 (2017).

[12] M. Puljiz, S. Huang, K. A. Kalina, J. Nowak, S. Odenbach, M. Kästner, G. K. Auernhammer, A. M. Menzel, Soft Matter **14**, 6809 (2018).

[13] M. Puljiz, A. M. Menzel, Phys. Rev. E **99**, 053002 (2019).

[14] L. Fischer, A. M. Menzel, Phys. Rev. Research **2**, 023383 (2020).

[15] A. M. Menzel, J. Chem. Phys. **154**, 204902 (2021).

[16] L. Fischer, A. M. Menzel, Smart Mater. Struct. **30**, 014003 (2021).

Microstructure guided constitutive modeling of isotropic compressible magneto-active polymers at the macroscale level

P. Gebhart, Th. Wallmersperger

Institute of Solid Mechanics, Technische Universität Dresden, 01062 Dresden, Germany

In recent years there has been an increasing interest in the theoretical and experimental study of field-responsive composite materials. Magneto-active polymers (MAPs) are a special class of field responsive solids that comprise of a polymeric matrix with dispersed micro-sized magnetizable particles. As a result of this microstructural composition, these materials deform and alter their material characteristics under the influence of magnetic fields. These properties in combination with the tunability of specific characteristics through the fabrication process makes them attractive for various engineering applications. Experimental and numerical investigations have shown that the magneto-mechanical behavior of MAPs at the macroscale level strongly depends upon the macrostructural shape of the body [1, 2]. This fact poses a crucial challenge in the accurate experimental determination of the effective material properties of the composite material. In this work we make use of an energy-based computational framework embedded into a scale transition scheme to bridge between micro- and macroscale and compute the homogenized macro-response of the underlying microstructure. This methodology allows the in silicio generation of a comprehensive data set and overcomes the inherent difficulties in the experimentally based material characterization of MAPs. We outline ingridients of the constitutive theory in an energy-based arrangement and develop - guided by the comprehensive homogenization data - specific constitutive expressions that are able to accurately capture the highly nonlinear material response of MAPs at the macroscale level. Moreover, we propose an elegant three-level fitting algorithm for the precise parameter identification based on the in silicio generated homogenization data set and discuss polyconvexity of the developed constitutive model. The validity and accuracy of the developed macroscale model is demonstrated by solving some application-oriented boundary value problems along with the application of a micro-macro decoupling scheme. The main emphasis of the numerical studies lies on the investigation of the magnetostrictive and magnetorheological effect at the macroscale level.

Acknowledgments

This research has been financially supported by the Deutsche Forschungsgemeinschaft in the framework of the Priority Programme SPP1681.

References

[1] K. Kalina, Mehrskalige Modellierung und Finite-Elemente-Simulation magnetorheologischer Elastomere, Dissertation, TU Dresden, 2021.

[2] P. Gebhart and T. Wallmersperger, A constitutive macroscale model for compressible magneto-active polymers based on computational homogenization data: Part I - Magnetic linear regime, IJSS, 2021, submitted.

Density functional theory for a three-dimensional model of ferrogels

S. Goh[1], A. M. Menzel[2], R. Wittmann[3], H. Löwen[3]

[1]*Theoretical Physics of Living Matter, Institute of Biological Information Processing, Forschungszentrum Jülich, 52425 Jülich, Germany*
[2]*Institut für Physik, Otto-von-Guericke-Universität Magdeburg, Universitätsplatz 2, 39106 Magdeburg, Germany*
[3]*Institut für Theoretische Physik II: Weiche Materie, Heinrich-Heine-Universität Düsseldorf, Universitätsstraße 1, 40225 Düsseldorf, Germany*

Background

Magnetorheological gels and elastomers [1], henceforth referred to as ferrogels, are composite materials whose elastic properties are controllable by the application of external magnetic fields. While such a composite nature gives rise to rich magnetostrictive effects as well as external-field dependent elastic moduli, the theoretical description of ferrogels is challenging due to their genuine multi-scale characteristics. In this study, we aim at understanding the statistical mechanics of ferrogels. On the one hand, our approach provides a scale-bridging description [2], specifically across the meso- and macroscopic scales. On the other hand, thermal fluctuations of magnetic particles are automatically included, which have been largely neglected so far in mesoscopic descriptions, in spite of their frequent relevance in soft matter systems in general. To this end, we further develop a description in terms of density functional theory (DFT), the first steps towards which have been outlined in previous studies [3]. In particular, we extend the approach to three dimensions. This requires to resolve certain technical and conceptual challenges but is essential in developing a theory appropriate for the characterization of actual materials.

Model and theory

We use a mesoscopic dipole-spring model as a basis and reference to develop DFT for ferrogels. It addresses magnetic particles connected by harmonic springs. In this model, magnetic particles are distinguished by their positions as they are trapped by the network of harmonic springs (or by the elastic matrix in reality). In density functional theory, however, particles are assumed to be indistinguishable. To overcome this discrepancy, we here constrain ourselves to regular, crystal-like spatial arrangements of indistinguishable magnetic particles subject to a pseudo-spring pair potential, in place of the original harmonic springs persistently connecting prescribed particle pairs. This step effectively renders the magnetic particles distinguished in the theoretical description, although in reality they are trapped according to their localized positioning. The pseudo-spring potential is then fine-tuned so that the resultant lattice structure agrees with the prescribed connectivity of the considered regular lattice arrangement. Here we investigate face-centered cubic (FCC) lattices, the (0,0,1)- or (1,1,1)-orientations of which are aligned along the direction of the magnetic dipoles carried by the particles. We consider all dipoles to be aligned along the same direction, as prescribed, for instance, by a strong external magnetic field.

Issues to be addressed

First, the strong external magnetic field tends to fix the regular lattice along specific orientations. Therefore, coefficients

of relative rotations between the anisotropic particle structure and the direction of their magnetization need to be calculated explicitly. In other words, the external magnetic fields here break rotational symmetry explicitly [4]. Second, many ferrogel systems are virtually incompressible and thus, there is a demand for a discretized statistical theory capable of addressing elasticity under constraints such as preserved volume [5].
Third, in contrast to the one- and two-dimensional cases [3], the magnetic field necessarily distinguishes one specific direction within the space. Therefore, magnetostrictive effects affect both the volume and shape of the systems, which we determine within our DFT calculations. Fourth, in three dimensions, the magnetic dipole-dipole interaction is marginally long-ranged and, therefore, the total magnetic energy depends on the shape of the investigated samples. We also address this issue by calculating the corresponding long wavelength mode in Fourier space.

Results

We first address magnetostrictive effects, that is, deformations upon magnetization of our model systems [6]. In particular, we confirm that the system response critically depends on the spatial arrangement of the magnetic particles. Specifically, for stronger magnetic interactions, elongation along the field direction is observed in the (0,0,1)-case. In contrast to that, we observe contraction along the magnetic field direction when the magnetic dipoles are oriented along the (1,1,1)-axis of lattice.
We then calculate elastic constants and rotation coefficients [6]. Once again, it is confirmed that the resultant values depend on the spatial configuration of magnetic particles. Moreover, our DFT calculation reveals a softening of the lattice structures along the direction of the magnetic field and in the plane perpendicular to this direction. The associated instabilities at elevated magnetic interaction strengths may indicate a destabilization of the initial lattice arrangement and the formation of a hexagonal-like arrangement as well as touching magnetic particle-pairs, respectively. This aspect needs additional investigation and further clarification in the future.

Acknowledgments

This work was supported through funding by the Deutsche Forschungsgemeinschaft via the SPP 1681, grant nos. ME 3571/3 (A.M.M.) and LO 418/16 (H.L.).

References

[1] S. Odenbach, Arch. Appl. Mech. **86**, 269 (2016); R. Weeber, P. Kreissl, and C. Holm, Arch. Appl. Mech. **89**, 3 (2019); A. M. Menzel, Arch. Appl. Mech. **89**, 17 (2019).

[2] A. M. Menzel, J. Chem. Phys. **141**, 194907 (2014); G. Pessot *et al.*, J. Phys.: Condens. Matter **27**, 325105 (2015); A. M. Menzel and H. Löwen, Phys. Sci. Rev., 20190088 (2020); A. M. Menzel, J. Chem. Phys. **154**, 204902 (2021).

[3] P. Cremer, M. Heinen, A. M. Menzel, and H. Löwen, J. Phys.: Condens. Matter **29**, 275102 (2017); S. Goh, R. Wittmann, A. M. Menzel, and H. Löwen, Phys. Rev. E **100**, 012605 (2019).

[4] S. Bohlius, H. R. Brand, and H. Pleiner, Phys. Rev. E **70**, 061411 (2004); A. M. Menzel, J. Chem. Phys. **141**, 194907 (2014).

[5] S. Goh, H. Löwen, and A. M. Menzel, in preparation.

[6] S. Goh, R. Wittmann, A. M. Menzel, and H. Löwen, in preparation.

Magnetic nanoparticles pass an *in vitro* blood-placenta barrier under continuous flow conditions

L.J. Gresing[1], M. Sutter[1], P. Radon[2], A. Weidner[3], R.P. Friedrich[4], S. Dutz[3], C. Alexiou[4], F. Wiekhorst[2], A. Hochhaus[1], J.H. Clement[1]

[1] *Klinik für Innere Medizin II, Abt. Hämatologie & Internistische Onkologie, Universitätsklinikum Jena, Am Klinikum 1, D-07747 Jena, Germany; mail to: joachim.clement@med.uni-jena.de*
[2] *Physikalisch-Technische Bundesanstalt, Berlin, Germany*
[2] *Institut für Biomedizinische Technik und Informatik (BMTI), Technische Universität Ilmenau, Germany*
[4] *Hals-Nasen-Ohren-Klinik, Abt. SEON, Universitätsklinikum Erlangen, Germany*

Introduction

Nanotechnology and the application of nanomaterials have been rapidly progressing within the past years. Thus, there is an urgent need to study the interaction between nanomaterials and the human body especially at cellular interfaces. Since clinical trials on pregnant women are difficult to perform, there is a strong necessity for physiologically appropriate models of the human placenta to study nanoparticle-placenta interactions *in vitro*. During pregnancy, the placenta delivers nutrients from the maternal blood to the fetus and metabolites in reverse direction. This organ is also responsible for the protection of the fetus from harmful substances. The blood-placenta barrier (BPB) is formed by various cell types, especially by trophoblasts and endothelial cells, placental macrophages (Hofbauer cells) and pericytes. The aim of our investigations is to gain a better understanding of the interactions of nanomaterials, especially magnetic nanoparticles (MNP), with the blood-placenta barrier [1]. Recently, we transferred the *in vitro* blood-placenta model from the transwell setup to a microfluidic biochip. In the present study, we investigate the interaction of different magnetic nanoparticles under fluidic conditions with a special focus on extended incubation times, the passaging abilities of the MNPs and the putative changes in the production of pro- and anti-inflammatory cytokines.

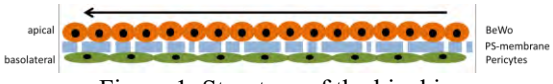

Figure 1. Structure of the biochip

Materials and Methods

The *in vitro* blood-placenta barrier was formed by the seeding of 200,000 BeWo cells (human trophoblast-like cell line, derived from a choriocarcinoma [2]) into the upper channel of the biochip and a 24h-incubation at 37°C, 5% CO_2 in a humidified atmosphere (Fig. 1).

Next, 350,000 human placental pericytes were seeded into the lower channel and incubated for another 48 h at the same culture conditions. For incubation under continuous flow, the biochip was connected to a peristaltic pump and the barrier was cultured for additional 96 h with laminar flow at a flow rate of 44 µL/min. DMEM +15% FCS +1% Pen/Strep was used as culture medium in all experiments. Molecular permeability assays using sodium fluorescein (NaFlu) were conducted to prove cell barrier integrity prior to MNP incubation as well as immunofluorescence staining of the tight junction-associated protein ZO-1 of BeWo cells. 4 different magnetic iron oxide nanoparticles were used with a final concentration of 100 µg/mL:

	NaZ	CA	SEON	PEI-M
Core	maghemite	maghemite	magnetite	magnetite
Shell	sodium citrate	citric acid	lauric acid + HSA	polyethylen imine
Hydro. Diameter	116 nm	78 nm	97 nm	150 nm
ζ-potential	-35.4 mV	-28.4 mV	-21.3 mV	54.0 mV
	AG Dutz	AG Dutz	AG Alexiou	Micromod

Cytokine profiling was performed by applying the LEGENDplex inflammation assay (BioLegend) including 13 cytokines. Magnetic particle spectroscopy (MPS) was

used for MNP-specific iron quantification upon MNP incubation. For MPS, the third harmonics of the spectra were normalized to the moment of a MNP reference sample of known iron amount.

Results and Discussion

BeWo cells co-cultured with pericytes form a stable barrier inside the microfluidic biochip, confirming the observations from the static transwell system [1]. The formation of the barrier significantly reduced the permeability of the membrane for sodium fluorescein in comparison to blank (46.2 vs. 345 nM NaFlu). The incubation of the biochip with or without laminar flow does neither affect the expression of the tight junction protein Zonula occludens-1 nor the overall cell morphology [3]. The applied MNPs neither reduce the viability of BeWo cells in 2D cell culture nor disrupt the cell barrier on the biochip.

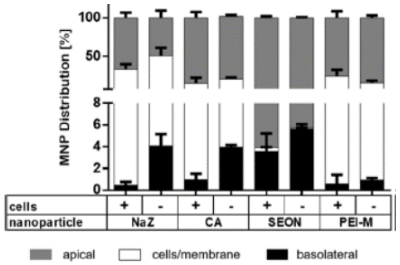

Figure 2: Passage of different nanoparticles in the BPB model quantified by MPS.

After 7 days of incubation, the reservoir of the biochip was filled with 800 µl nanoparticle-solution as indicated in standard medium. The NP-solution circulated for 24h through the upper channel of the biochip. The flow-through was collected in one sample (apical). Subsequently, the medium of the lower channel (basolateral) was collected and the membrane containing the cell layers (cells/membrane) was cut out. All samples were analyzed using MPS. The relative concentrations were calculated from the obtained absolute values. [3]

The passage of the MNPs through the barrier was monitored by MPS after anincubation time of 24h. The distribution within the upper channel, the lower channel and the membrane was MNP-specific (Fig. 2). More than 65% of nanoparticles remain in the upper channel, but 33% (± 6.5% SD) of NaZ accumulate in the cell layers and 3.5% (± 1.65%) of SEON particles reach the lower channel. In order to exclude inflammatory effects of MNPs we studied the secretion of a panel of 13 pro- and anti-inflammatory cytokines after a 24h-incubation of the fluidic blood-placenta barrier with MNP. IL-6, IL-8 and MCP-1 were the predominant cytokines in the system. In general, the cytokine concentration was higher on the apical side than on the basolateral side. That might be due to the continuous circulation of the medium on that side. After the 24 h-incubation, the levels of the investigated cytokines were unchanged in comparison to controls without MNP application. As expected, the toxin Lipopolysaccharide caused a 10- to 20-fold increase of IL-6, IL-8 and MCP-1 concentration on the apical side.

Conclusion and Outlook

We could demonstrate that BeWo cells co-cultured with pericytes form a stable barrier inside the microfluidic biochip. MPS allows a precise determination of the nanoparticle concentrations in the different compartments of the biochip. The capability of MNPs to pass the barrier depends on their surface composition. Anionic MNPs do not affect the inflammation-related cytokine profile. Future work will focus on the differentiation of the trophoblasts to allow MNP-cell interaction in a dynamic biological context.

Acknowledgement

We thank Cornelia Jörke for expert technical assistance and Martin Raasch and Alexander Mosig (Inst. Biochemistry II, FSU Jena) for substantial support with the biochips. This work was supported by Deutsche Forschungsgemeinschaft (DFG) in the framework of the priority program 1681 (CL202/3-3, DU1293/7-3, WI4230/1-3, AL552/5-3).

References

[1] E. K. Müller et al., *Nanomat.* 2018, *8, 108*
[2] R. A. Pattillo and G. O. Gey, *Cancer Res* 1968, *28:1231-1236*
[3] L. Gresing et al., *J Magn Magn Mater* 2021; *521: 167535*

Surface engineering and stable dispersions of magnetic nanoparticles in a nematic liquid crystal

M. Hähsler[1], S. Behrens[1]

[1] *Institute of Catalysis Research and Technology, KIT, Karlsruhe, Germany*

Hybridization of magnetic nanoparticles (MNPs) with liquid crystals (LC) opens new opportunities for the development of novel magneto-responsive materials and devices, e.g. for transparent magnets, actuators, sensors, data storage etc.[1,2] However, embedding MNPs in LC matrices is far from trivial with MNP aggregation to complete phase separation. Here, we show the synthesis of MNPs with shape (an)isotropy [3,4,5] and their integration in MNP-LC hybrid materials with long-term colloidal stability [5]. The key feature in the design of these materials is the functionalization of the MNPs with (pro)mesgenic ligands, allowing an effective coupling between the MNPs and the LC matrix.

In a first step, the synthesis of MNPs with different sizes and (an)isotropic shapes (Fig. 1) *via* thermal decomposition and hydrothermal processes was addressed. Fig. 1 displays a selection of MNPs of various materials, sizes and shapes. For example, $BaFe_{12}O_{19}$ nanoplatelets were received *via* hydrothermal synthesis where the size was controlled by reaction temperature and the magnetic properties *via* metal doping (e.g. Sc, In, Ga) [4]. The structure and magnetic properties were analyzed, e.g., by electron microscopy (SEM / TEM), XRD, thermal gravimetric analysis (TGA), IR and Raman spectroscopy, inductively coupled plasma - optical emission spectroscopy (ICP-OES), Mössbauer spectroscopy, and alternating gradient magnetometry (AGM). Zero-field-cooling (ZFC) and field-cooling curves (FC) were measured for selected samples on a superconducting quantum interference (SQUID) device.

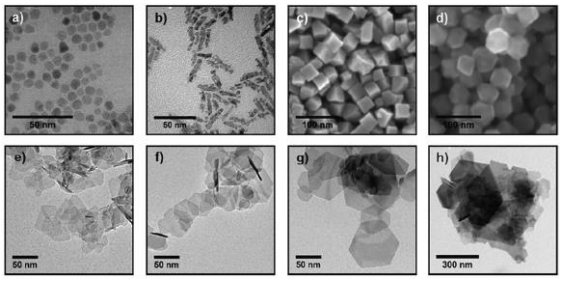

Figure 1. TEM or SEM images of (a) spherical $Co_{0.6}Fe_{2.4}O_4$ MNPs, (b) Fe_3O_4 nanorods, (c) Fe_3O_4 nanocubes, (d) Fe_3O_4 cuboctahedra and (e)–(h) Sc-doped barium $BaFe_{12}O_{19}$ nanodiscs. The higher the reaction temperature was, the bigger the as-formed nanodiscs were: (e) 210 °C, (f) 260 °C, (g) 310 °C, and (h) 340 °C [5].

The interface between MNP and LC host (i.e. the surface properties of the MNPs) is of utmost importance (Fig. 2) [5]. Various types of (pro)mesogenic aliphatic and dendritic ligands have been designed by us over the last years consisting typically of 1) a functional group for MNP binding, which is linked by 2) a flexible spacer to 3) the mesogenic unit [6]. It should be noted that MNP functionalization requires ligand exchange procedures which are specific to both the type of MNP and the ligand. The nature of the ligand, the MNP size and shape critically influences the colloidal stability of the MNPs and their coupling to the surrounding LC matrix. Fig 2. illustrates the critical influence of the ligand structure on MNP stability in the nematic 5CB phase. Mesogenic ligands with either octylbiphenyl or cyanobiphenyl group but otherwise similar structure revealed a significantly different behavior when immersed in 5CB.

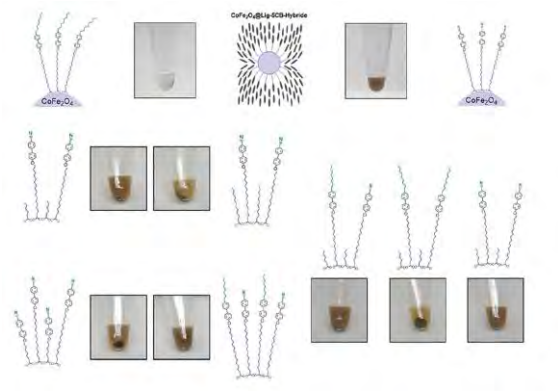

Figure 2. Influence of the end group on the biphenyl moiety of the ligands on the stability of the MNPs in 5CB illustrating the importance of MNP-matrix interactions in these systems and the need for a highly specific surface engineering of the MNPs [5].

In particular, mesogenic ligands with dendritic structure ensure colloidal stability also for bigger MNPs in 5CB [7]. Spherical $CoFe_2O_4$@dend MNPs integrated in 5CB resulted in a hybrid material behaving macroscopically like a ferrofluid. Dendronized MNPs reveal also a shape-dependent stability in 5CB (Fig. 4).

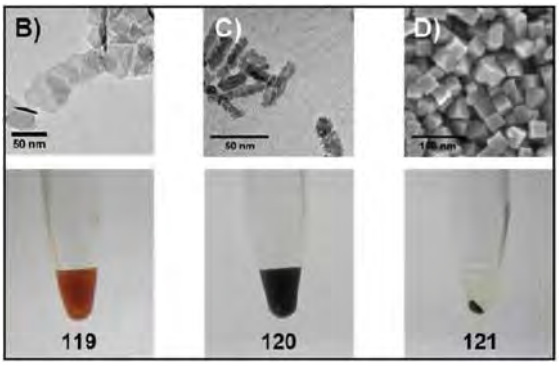

Figure 3. Shape-dependent stability of dendronized MNPs in 5CB [8].

The coupling of the MNP subphase and the magneto- and electro-optical behavior were studied for stable dispersions of 4.6 nm, dendronized $CoFe_2O_4$ MNPs in 5CB in collaboration with A. Eremin (Univ. of Magdeburg) [7, 8]. The unusual magneto-optical behavior seems to be due to the topologically controlled self-assembly of chain-like MNP structures in 5CB.

Acknowledgments

The financial support by the German Science Foundation (DFG) within the Priority Program "Field controlled particle matrix interactions: Synthesis, multiscale modeling and application of magnetic hybrid materials" (SPP1681; projects BE 2243/3 and STA 425/36) is gratefully acknowledged.

References

[1] A. Mertelj; D. Lisjak; M. Drofenik; M. Copic; Nature 2013, 504 (7479), 237-241.
[2] X. Liu; et al., Science 2019, 365, 264-267.
[3] M. Hähsler; J. Landers; T. Nowack; S. Salamon; M. Zimmermann; S. Heissler; H. Wende; S. Behrens; Inorg. Chem. 2020, 59, 3677−3685.
[4] M. Hähsler; M. Zimmermann; S. Heissler; Behrens; Journal of Magnetism and Magnetic Materials 500 (2020) 166349.
[5] M. Hähsler; I. Appel; S. Behrens; Phys. Sc. Rev. 2020, 20190090 eISSN 2365-659X.
[6] M. Hähsler; J. Gross; Behrens; Eur. J. Org. Chem. 2019, 7820–7830.
[7] M. Hähsler; H. H. Nádasi; M. Feneberg; S. Marino; F. Giesselmann; S. Behrens; A. Eremin; Adv. Funct. Mater. 2021, 2101847.
[8] M. Hähsler, Dissertation, Universität Heidelberg, 2020.

Continuum approaches for the modeling and simulation of magnetorheological elastomers

K. A. Kalina[1], P. Metsch[1], M. Kästner[1,2]

[1]*Chair of Computational and Experimental Solid Mechanics, TU Dresden, 01062 Dresden, Germany*
[2]*Dresden Center for Computational Materials Science (DCMS), TU Dresden, 01062 Dresden, Germany*

Magnetorheological elastomers (MREs) are a class of active composites consisting of a soft matrix filled with micron sized magnetizable particles. The effective properties of these materials essentially depend on the properties and the microstructural arrangement of the individual components. In order to investigate the behavior of MREs, a continuum based computational modeling approach is applied in this contribution [1].

Microscopic particle interactions

In a first part, field-induced interactions of magnetizable particles embedded into an elastomer matrix are analyzed with regard to the resulting mechanical displacements [2]. By comparing experimental data of particle-matrix systems with the results of finite element (FE) simulations, the applied continuum approach is validated. Thereby, the particle geometries and orientations within the simulations are taken from real CT-data.

Multiscale approach

In a second part, basic effective properties of MREs are analyzed by using a computational homogenization scheme. Exemplarily, the magnetorheological (MR)-effect of various microscopic particle arrangements is considered, where several influencing factors as the particle volume fraction or the direction of the applied magnetic field are analyzed systematically.
Finally, in order to enable the efficient simulation of macroscopic MRE samples and components, the development and calibration of a macroscopic model based on a microscopically generated data basis is shown [1]. Within these models, the composite is considered to be a homogeneous magneto-active continuum in which effects of the underlying microstructure are captured via coupling terms. With this model which is applicable for isotropic, magnetically soft and elastic MREs, simulations of the magnetostrictive (MS)- and MR-effects are performed.

Acknowledgments

The authors want to thank the groups of G. K. Auernhammer, G. J. Monkman and S. Odenbach for providing measurement data and CTs for the analysis of microscopic particle interactions. The present study is funded by the German Research Foundation, Priority Program (SPP) 1681 grants KA 3309/2-1/3. This support is gratefully acknowledged.

References

[1] Kalina, K. A.; Raloff, A.; Wollner, M.; Metsch, P.; Brummund, J. & Kästner, M.: *Physical Sciences Reviews* (2020).

[2] Metsch, P.; Schmidt, H.; Sindersberger, D.; Kalina, K. A.; Brummund, J.; Auernhammer, G. K.; Monkman, G. J. & Kästner, M.: *Smart Materials and Structures* 29.8 (2020).

Studying the Coupling Mechanisms in Nano-Rheological Soft Magnetic Systems Using Computer Simulations

P. Kreissl, Ch. Holm, R. Weeber

Institute for Computational Physics, University of Stuttgart, Allmandring 3, 70569 Stuttgart, Germany

Soft magnetic systems consist of magnetic nano-/micro-particles embedded in a polymeric environment. The particles' magnetic properties couple to the viscoelastic properties of their surroundings, which makes it possible to indirectly obtain local mechanical properties by measuring the system's dynamic magnetization response. The focus of our research is to use simulations for the study of these coupling mechanisms, the details of which are unfortunately, in many materials, still unknown.

Simulation Model

Our model uses molecular dynamics (MD) simulations [1]. Polymers in the system are represented using bead–springs, where monomers are connected with harmonic springs and a purely repulsive (WCA) potential is used to model excluded volume interactions. Hydrodynamics are solved using the efficient lattice-Boltzmann algorithm. Magnetic particles are modeled as so-called 'raspberry-particles' [2] – to provide proper coupling of both translational and rotational behavior to the fluid, the particle is represented as a rigid body consisting of homogeneously distributed fluid coupling points. The parameters for our simulations are based on the experimental system of Ref. [3].

Frequency-Shifts in the AC-Susceptibility

Typically, the dynamic response of a magnetic suspension to an applied magnetic field is non-linear. However, in the limit of small excitations linear response theory can be used. It provides the so-called Green-Kubo (GK) relations [4] – mathematical expressions that connect transport coefficients to time correlation functions. We use the following relation to obtain AC susceptibility spectra from the time autocorrelation function of a system's (steady-state) magnetization $\vec{M}$,

$$\chi(\omega) = \frac{1}{V k_{\mathrm{B}} T} \left(\langle \vec{M}(0)\vec{M}(0)\rangle - \mathrm{i}\omega \int_0^\infty \exp(-\mathrm{i}\omega \mathrm{t}) \langle \tilde{\mathrm{M}}(\mathrm{t})\tilde{\mathrm{M}}(0)\rangle \, \mathrm{dt} \right), \quad (1)$$

with V the simulated box volume and $k_{\mathrm{B}}T$ the thermal energy.

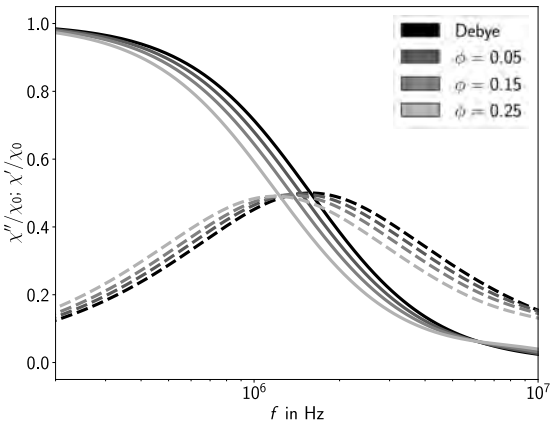

Figure 1: AC susceptibility obtained using the GK relation (Eq. 1), for polymers with chain length $N = 15$. Increasing the polymer volume fraction ϕ results in a shift towards lower frequencies [1].

For both increasing polymer volume fraction (see Fig. 1) and polymer chain length, respectively, we observe a shift of the AC susceptibility spectra towards lower frequencies [1], which is in line with experimental

observations [3]. In our simulations, solely hydrodynamic interactions couple the rotational behavior of the magnetic particle (and thus its magnetization response) to the surrounding polymer matrix. Given that this coupling alone reproduces the experimentally observed trends, hydrodynamic interactions proof to be a key element for nanorheological systems.
We are currently extending our model to investigate anisotropic particles, which introduces additional steric interactions.

Obtaining Elastic Properties

AC susceptibility spectra can be used to extract local elastic properties via appropriate theoretical models [3], such as the Gemant-DiMarzio-Bishop (GDB) model. For example, the loss modulus is given as

$$G''(\omega) = \frac{1}{K} \frac{\chi''_{\mathrm{N}}}{(\chi'_{\mathrm{N}})^2 + (\chi''_{\mathrm{N}})^2}, \qquad (2)$$

with $K = 4\pi a^3/(k_{\mathrm{B}}T)$ and $\chi''_{\mathrm{N}} = \chi''/(\chi_0 - \chi_\infty)$. Fig. 2 shows examples for loss moduli calculated from AC susceptibility spectra.

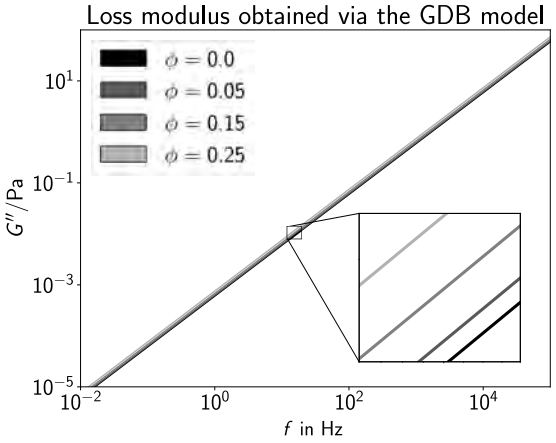

Figure 2: Loss modulus G'' calculated from the AC susceptibility spectra of Fig. 1 using the GDB model (Eq. 2). With increasing volume fraction, a monotonous increase of the loss modulus is observed.

While the aforementioned method primarily probes the local environment of the magnetic particle, we can also obtain the global

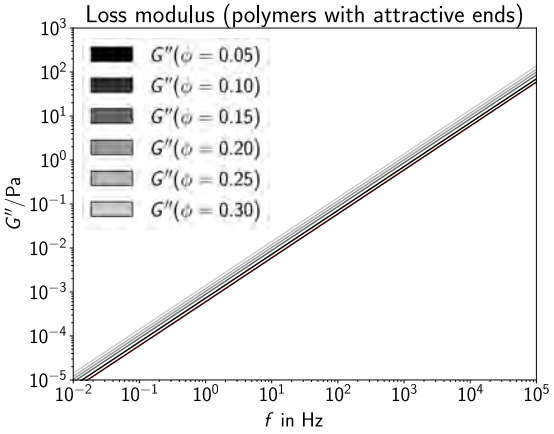

Figure 3: Loss modulus obtained using the GK relation for the stress tensor (Eq. 3). The polymers have the length $N = 25$ and there is an attractive interaction between all chain-ends, which leads to a more pronounced coupling with increasing volume fraction.

elastic moduli using a GK relation on a simulation system without magnetic particles,

$$G = \frac{V}{k_{\mathrm{B}}T} \langle \sigma_{xy}(t)\sigma_{xy}(0) \rangle, \qquad (3)$$

where σ_{xy} are the off-diagonal elements of the stress tensor (see Fig. 3).

Acknowledgments

The authors are grateful for funding by the DFG through the SPP 1681.

References

[1] P. Kreissl, C. Holm and R. Weeber, Soft Matter 17, 147–183, 2021.

[2] L. P. Fischer, T. Peter, C. Holm and J. de Graaf, J. Chem. Phys. 143, 084107, 2015.

[3] E. Roeben, L. Roeder, S. Teusch, M. Effertz, U. K. Deiters and A. M. Schmidt, Colloid Polym. Sci. 292, 20132023, 2014.

[4] R. Kubo, J. Phys. Soc. Jpn. 12, 570586, 1957.

Ferromagnetic nematics in rotating and oscillating magnetic fields

M. Küster[1], H. Nádasi[2], N. Sebástian[3], P. H. Boštjančič[3], D. Lisjak[3], A. Mertelj[3], A. Eremin[2], F. Ludwig[1]

[1] *Institut für Elektrische Messtechnik und Grundlagen der Elektrotechnik und LENA, TU Braunschweig, Braunschweig, Germany*
[2] *Institut für Physik, ANP, Otto-von-Guericke-Universität Magdeburg, Magdeburg, Germany*
[3] *J. Stefan Institut, Ljubljana, Slovenia*

Introduction

Soft magnetic materials, such as magnetic fluids, gels and elastomers, have recently come into focus of intensive research. The ability to easily manipulate optical and mechanical properties makes them essential components for designing intelligent materials. Recently, Mertelj et al. demonstrated that dispersions of magnetic nano-platelets in liquid crystals could exhibit ferromagnetic order [1,2]. Liquid crystalline order is expected to profoundly affect the dynamics of the magnetic particles, which is still not fully understood. Here, we report the study of magnetization dynamics and the magnetomechanical effect of a colloidal dispersion of barium hexaferrite nano-platelets in rotating and oscillating magnetic fields.

Experiment

Scandium-doped barium hexaferrite (BaHF) nano-platelets with DBSA surfactant [1] were suspended in isotropic 1-butanol with nominal concentrations of 10 mg/mL (SP10), 30 mg/mL (SP30), 181 mg/mL (SP181) and 347 mg/mL (SP347). The magnetic moment of these nano-platelets is directed perpendicularly to the basal plane. The sample with the highest BaHF nano-platelet concentration (SP347) exhibits nematic order. To estimate the nano-platelet size and magnetic moment, magnetization vs. magnetic field measurements were performed using a MPMS-3 from Quantum Design. From the saturation magnetization $M_s = 31.3$ Am^2/kg, measured on SP10, and the volume, estimated from TEM images, a magnetic moment $m = 1.7 \cdot 10^{-18}$ Am^2 was estimated. The dynamics of the BaHF platelets is studied using AC susceptometry in a frequency range from 0.1 Hz - 9 kHz and for field amplitudes up to 5 mT. The magnetomechanical effect is studied in a spherical cavity suspended on a torsional balance for field amplitudes up to 0.5 mT.

Results

For the most diluted BaHF nano-platelet sample (SP10) we observe in the ac susceptibility (ACS) spectra three relaxation modes (Fig. 1). Fitting the characteristic frequency of the high-frequency mode as a function of field amplitude with the model by Yoshida and Enpuku [3] we estimated a magnetic moment of $m = 4.3 \cdot 10^{-18}$ Am^2, in fair agreement with the value given above. Thus, this mode is attributed to the relaxation of individual nano-platelets. The other two modes are caused by the collective motion of nano-platelets. For the nematic BaHF sample (SP347), only one, slightly asymmetric maximum is discernable. The slight asymmetry indicates the existence of at least two relaxation modes. The maximum of the imaginary part at a field amplitude of 0.5 mT occurs at a characteristic frequency of 53 Hz, which is much lower than that of the high-frequency peak of SP10 (593 Hz).

Magnetomechanical measurements with the torsion balance (TB) provide for the low-concentration samples SP10 and SP30 spectra that are proportional to the measured ACS imaginary parts (Fig. 2). This is in

good agreement with the model by Torres-Diaz and Rinaldi [4], which proposes that the torque density N_V is given by

$$N_V \propto H_0^2 \chi''$$

with magnetic field amplitude H_0 and ACS imaginary part χ''. Moreover, the conversion efficiency of the magnetic torque into the mechanical is particularly strongly pronounced in our system since the Néel relaxation mechanism is suppressed. The origin of the magnetomechanical torque is the vortex flow sustained by rotating MNPs.

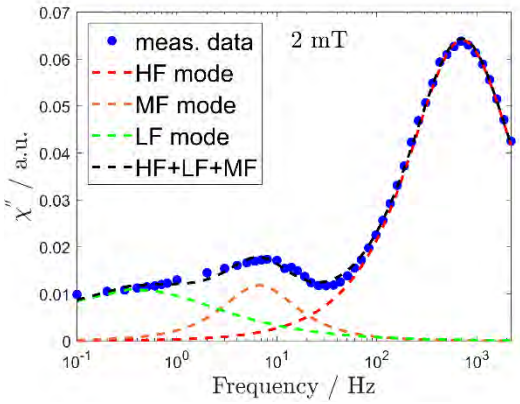

Figure 1. AC susceptibility imaginary part measured on SP10 for 2 mT field amplitude. Dashed lines depict fits with three relaxation modes.

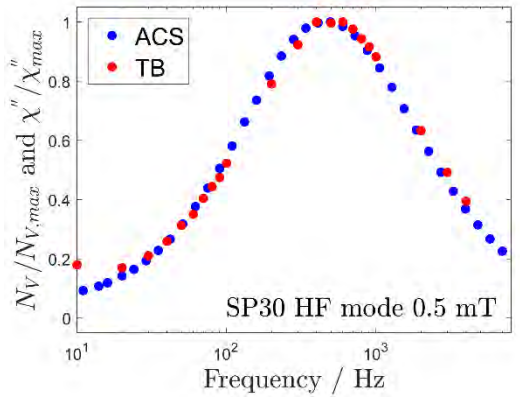

Figure 2. Comparison of normalized TB spectrum and normalized imaginary part of ACS measured on sample SP30 at 0.5 mT field amplitude.

Conclusion and outlook

The dynamic measurements on differently concentrated BaHF suspensions show distinct differences. In all cases, several relaxation modes were observed in ACS as well as in torsional balance measurements. While the high-frequency mode in the most diluted samples can be attributed to the rotational motion of individual nano-platelets, the mechanism behind the other modes is not clear yet and requires further investigations.

Our studies show that the magnetomechanical torque follows the same frequency behavior as the loss part of the ac susceptibility χ''.

The research was funded by DFG via projects LU 800/7-1 and NA 1668/1-1.

References

[1] A. Mertelj et al., “Ferromagnetism in suspensions of magnetic platelets in liquid crystal”, Nature 504, 237–241 (2014).

[2] N. Sebastián et al., “Director reorientation dynamics of ferromagnetic nematic liquid crystals”, Soft Matter 14, 7180-7189 (2018).

[3] T. Yoshida and K. Enpuku, “Simulation and quantitative clarification of ac susceptibility of magnetic fluid in nonlinear Brownian relaxation region”, Jpn. J. Appl. Phys. 48, 127002 (2009).

[4] I. Torres-Diaz and C. Rinaldi, “Ferrofluid flow in a spherical cavity under an imposed uniform rotating magnetic field: Spherical spin-up flow”, Phys. Fluids 24, 082002 (2012).

Magnetic response of $CoFe_2O_4$ nanoparticles confined in PNIPAM-microgel networks

J. Landers[1], M. Witt[2], J. Kopp[1*], S. Hinrichs[3], S. Salamon[1], B. Hankiewicz[3], R. von Klitzing[2], H. Wende[1]

[1] *Faculty of Physics and Center for Nanointegration Duisburg-Essen (CENIDE), University of Duisburg-Essen*
[2] *Department of Physics, Soft Matter at Interfaces, Technical University Darmstadt*
[3] *Institute of Physical Chemistry, Hamburg University*

Magnetic microgels based on magnetically blocked $CoFe_2O_4$ nanoparticles embedded in N-isopropylacrylamid (NIPAM) microgel particles exhibit versatile response behavior to external stimuli: They combine the characteristic NIPAM volume phase transition (VPT) at ca. 32°C with tunable response of the magnetic nanoparticles (MNPs) to applied magnetic fields dependent on the degree of constraint of the MNPs within microgel meshes.
Here, we utilize the distinct variation in PNIPAM mesh size upon rising temperature for an in-depth characterization of nanoparticle dynamics under effects of confinement via AC-susceptometry. For that purpose, microgels MMG1 with and MMG2 without allyl mercaptan (AM) modification were loaded with $CoFe_2O_4$ nanoparticles of 12.2 ± 3.2 nm in diameter. As visible in fig. 1, the nanoparticles are continuously dispersed in sample MMG1, while minor agglomerates of MNPs are present in AM-modified microgels.

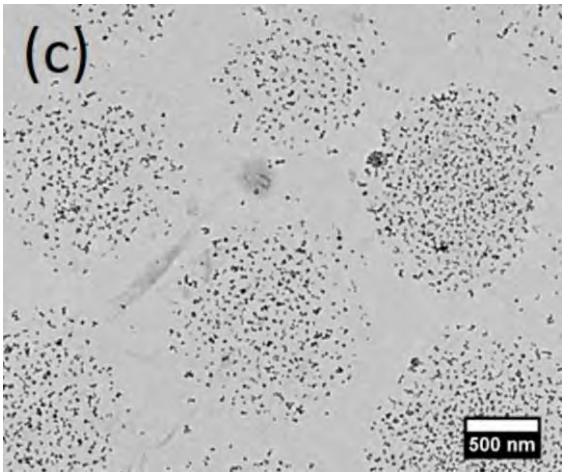

Fig. 1: TEM image of MNPs embedded in PNIPAM microgel particles (MMG1). [1]

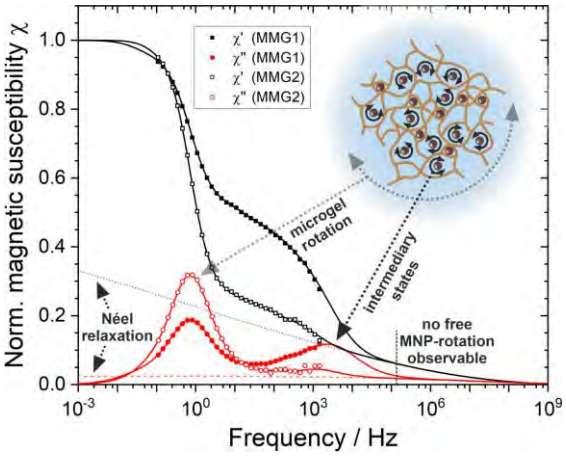

Fig. 2: Normalized magnetic susceptibility of regular (full) and AM-modified microgels (hollow symbols). Solid lines stem from the model described in the text, dashed lines represent the Néel relaxation background modeled for identical model parameters without Brownian motion. [1]

Average microgel diameters were found to be ca. 1.50 µm (MMG1) and 0.98 µm (MMG2), respectively and showed to be mainly unaffected under repeated cycling between 20°C and 50°C across the VPT.
Temperature-dependent magnetization measurements verified the MNPs to be almost completely magnetically blocked, therefore performing magnetic relaxation primarily via Brownian processes, directly reflecting the degree of particle confinement within meshes of the PNIPAM microgels. This is schematically demonstrated in fig. 2, showing the magnetic AC-susceptibility recorded at 20°C. Both MMG1 and MMG2 display particles tightly trapped in the PNIPAM gel, indicated by the presence of the peak in χ'' at ~ 1 Hz, corresponding to the microgel particle diameter, as microgel particle rotation is the only type of relaxation allowing a reor-

ientation of these MNP magnetic moments. While no signal of free MNP rotation is present at about 10^5 Hz, both samples exhibit distributions of intermediary states, where different degrees of MNP confinement affect their Brownian dynamics, which is more pronounced in regular microgels without added AM.

AC-susceptometry data have been modeled using a phenomenological model, describing Néel- and Brownian dynamics of MNPs of given core diameter and variable total diameter to reproduce the distribution of relaxation times resulting from confinement effects. Thereby we yield distributions of effective diameters $P(D_{eff})$ ranging from core diameters representing free MNP rotation across intermediary states to microgel diameters corresponding to completely trapped magnetic nanoparticles (Fig. 3). For both samples, the main component of $P(D_{eff})$ at ca. 1 µm displays a temperature dependent shift in D_{eff} due to the beginning VPT, while only in MMG1 intermediary values of D_{eff} are present. This signal component shifts to higher values of D_{eff} upon rising temperature, which can be explained by the contraction of

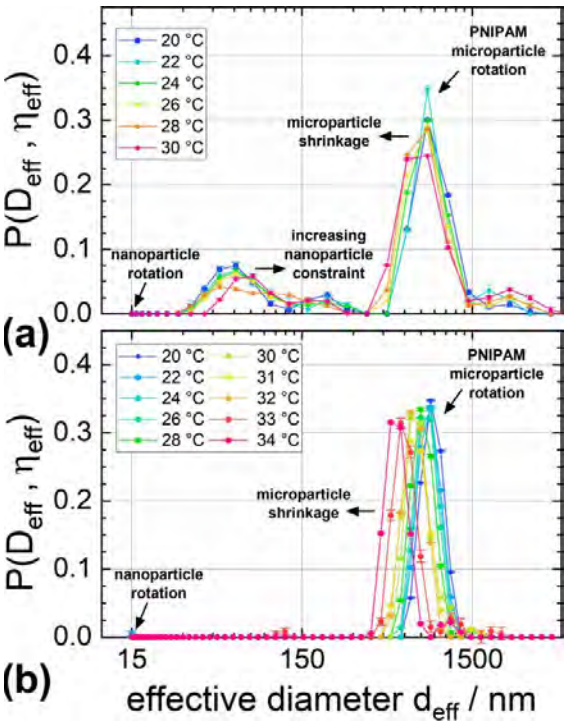

Fig. 3: Distributions of effective particle diameters (representing NP-confinement) extracted from AC-susceptometry for (a) regular and (b) AM-modified PNIPAM microgels. [1]

microgel meshes accompanied by enhanced MNP confinement. In MMG2, addition of AM leads to modified swelling of the microgel and to the formation of minor nanoparticle agglomerates, in combination resulting in the absence of partially free MNP rotation as seen in MMG1. The experiments verify the sensitivity of this approach to miniscule variations in MNP sizes and PNIPAM pores, respectively.

Acknowledgments

We gratefully acknowledge funding by the DFG through SPP1681 (grant WE2623/7-3, KL1165/18-1 and FI1235/2-2).

References

[1] M. Witt et al., submitted to Soft Matter

Mössbauer spectroscopy applied to soft magnetic hybrid materials

J. Landers[1], S. Salamon[1], J. Kopp[1], D. Günzing[1], S. Webers[1], H. Wende[1]

[1] *Faculty of Physics and Center for Nanointegration Duisburg-Essen (CENIDE), University of Duisburg-Essen*

Since its invention, Mössbauer spectroscopy (MS) has been a well-known technique for the non-destructive analysis of magnetic and chemical properties in solids. Shortly thereafter, this method was also applied to the detailed examination of magnetic nanostructures and nanoparticles (MNPs), as well as their Néel- and Brownian relaxation phenomena. [1] Here, we want to give a short overview on the ability to study different types of magnetic hybrid materials via MS, including ferrofluids, -hydrogels and -elastomers, as well as on the accessible physical properties.

In terms of ferrofluids, MS can provide information on nanoparticular Brownian motion in the regime of $D_T \approx 10^{-12} - 10^{-8}$ cm^2s^{-1}, resulting primarily in a distinct broadening of absorption lines proportional to the translational diffusion coefficient D_T and reduced spectral intensity (see Fig. 1). Based on this, nanoparticle core diameters and coating thickness could be inferred from temperature-dependent measurements for MNPs of 5 - 25 nm in glycerol solution. Simultaneously, MS allowed for the study of Néel relaxation times as well as the particle alignment, MNP cluster formation and surface spin canting, when the ferrofluids were exposed to magnetic fields. [2]

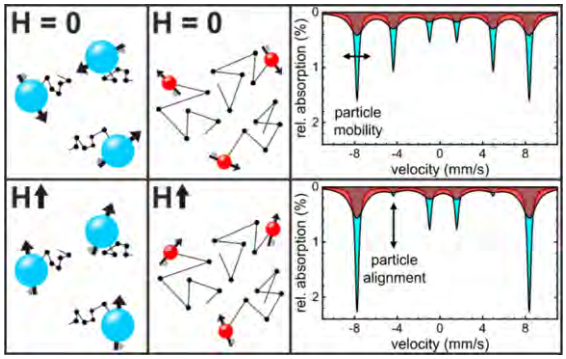

Figure 1. Effect of Brownian motion and in-field particle alignment in Mössbauer spectroscopy. [2]

Due to the time necessary to record a precise spectrum, MS is less often applied to time-dependent processes, although the time requirement can be drastically shortened by ^{57}Fe-enrichment. For that reason, when finding dramatic changes in magnetic particle alignment at phase transitions in ferrofluids, [3] AC-susceptometry and temperature-dependent magnetometry protocols were applied in combination with MS.

When the particles are embedded into polymeric networks in, e.g., ferrohydrogels, their motion is constrained to a degree determined by the local nanostructure of their surroundings. [4] This was studied utilizing hematite nanospindles in PAAm-hydrogels, where the acicular shape also enables the study of anisotropic effects. In this context, it's noteworthy that even after the onset of Brownian dynamics across the hydrogels' melting region, no significant motion was visible in AC-susceptometry experiments, although the particles still displayed considerable line broadening in MS. This could be explained in terms of the respectively studied timescale and the sensitivity to rotational (ACS) and translational dynamics (MS).

In ferroelastomers, nanoparticle movement is even further hindered, wherefore MS displays vibrational rather than Brownian line broadening. Here, the effect of strain as well as magnetic fields on the static nanoparticle orientation in the ferroelastomer was analyzed via MS complementarily to SAXS experiments. [5] It could be demonstrated that from relative absorption line intensities and nuclear quadrupole level shifts, not only the magnetic, but also the spatial particle orientation could be extracted.

Based on the wide range of magnetic nanoparticle characteristics accessible via MS applied to soft magnetic hybrid materials, we plan to focus more closely in the future on the effects of surrounding matrix material on MNP orientation phenomena. This will include the more detailed analysis of particle constraint dependent on the surrounding nanostructure. At the same time, the simultaneous examination of anisotropic particle motion and magnetic alignment shall be enabled via direction-resolved Mössbauer spectroscopy.

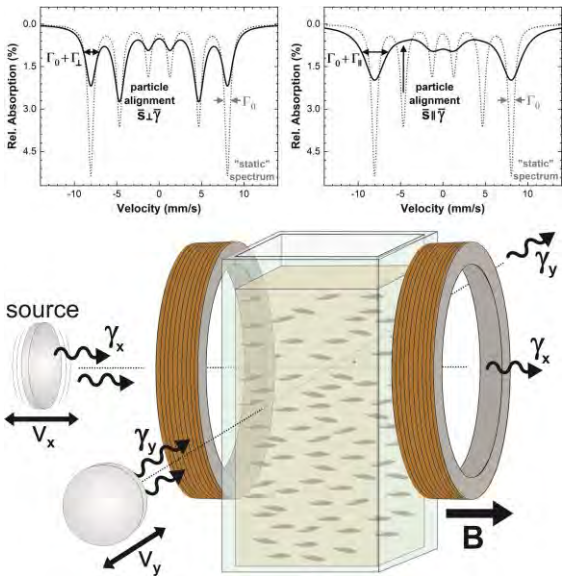

Figure 2. Schematic experimental setup for planned direction-resolved studies via MS. Spin alignment and anisotropy in particle diffusion relative to the γ-ray direction determine relative absorption line ratios and linewidths as shown in the simulated spectra: $\gamma \perp B$ (left) and $\gamma \parallel B$ (right).

Acknowledgments

We gratefully acknowledge funding by the DFG through SPP1681 (grant WE2623/7).

References

[1] Kündig et al. *Phys. Rev.* **142**, 327 (1966), Keller et al. *Solid State Commun.* **16**, 253 (1975)

[2] Landers et al. *Nano Lett.* **16**, 1150 (2016), Landers et al. *Appl. Mater. Interfaces* **11**, 3160 (2018)

[3] Webers et al. *Appl. Polym. Mater.* **2**, 2676 (2020)

[4] Plachinda et al. *Hyperfine Interact.* **56**, 1483 (1990), Landers et al. *J. Phys. Chem. C* **119**, 20642 (2015),

[5] Seifert et al. *Soft Matter* **17**, 7565 (2021)

Collective behavior of active colloids with dipolar (magnetic or electric) interactions

G.-J. Liao[1], S. H.L. Klapp[1]

[1]*Institute of Theoretical Physics, Technical University Berlin, Hardenbergstrasse 36, 10623 Berlin*

In recent years, the dynamical behavior of "active" (or "self-propelled") particles that can convert energy from an internal source or the surroundings into motion, has become a major focus in statistical physics and soft matter sciences. Indeed, it is now well established that active motion, combined with different types of particle-particle interaction, can lead to remarkable collective behavior such as motility-induced phase separation, swarming, and vortex formation. A standard model of active motion is the "active Brownian particle", where each particle moves with a constant propulsion speed along a direction subject to white noise, and the interactions are purely steric and isotropic. Here we consider, as an extension of that model, active particles with dipole-dipole interactions stemming from intrinsic (permanent) dipole moments or dipoles induced by an electric or magnetic field. Realistic examples include ferromagnetic "rollers" confined to a fluctuating surface which may exhibit swarming or vortex patterns when energized by a vertical alternating field [1], magnetotactic bacteria [2], and active metallodielectric Janus particles [3, 4].

To study the collective behavior of dipolar active particles, we have performed Brownian Dynamics (BD) simulations in two dimensions. In the first part of the talk, we focus on systems with active propulsion, where the propulsion direction of each particle is chosen to be parallel to its dipole moment. Already small clusters of such particle show intriguing behavior [5]. Here we consider large ensembles at a wide range of motilities and dipolar coupling strengths [6]. At low densities and low motilities, the most important structural phenomenon is the aggregation of the dipolar particles into chains, very similar to conventional (passive) dipolar particles. Upon increasing the particle motility, these chain-like structures break, and the system transforms into a weakly correlated isotropic fluid. At high densities, we observe that the motility-induced phase separation known from non-dipolar active particles is strongly suppressed by the dipolar coupling. Once the dipolar coupling dominates the thermal energy, the phase separation disappears, and the system displays a ferromagnetic "flocking" state, where particles form giant clusters and move collective along one direction. We provide arguments for the emergence of the flocking behavior, which is absent in the passive dipolar system. In the second part we turn to chiral active particles with dipolar interactions. Each particle is driven by both, translational propulsion (parallel to its intrinsic dipole moment) and rotational self-propulsion. Simulations are performed at high dipolar coupling strength and a moderate density. Despite this restriction, our simulations reveal a wealth of phenomena including formation of two types of vortices, phase separation, and flocking transitions [7]. We close by discussing challenges for an accompanying theoretical description (see, e.g., [8]) and further open questions.

Acknowledgments

We gratefully acknowledge financial support

by the German Research foundation via SPP 1681
and IRTG 1524.

References

[1] A. Kaiser, A. Snezhko and I. S. Aranson, Sci. Adv., 2017, 3, e1601469.

[2] F. Meng, D. Matsunaga and R. Golestanian, Phys. Rev. Lett., 2018, 120, 188101.

[3] S. Gangwal, O. J. Cayre, M. Z. Bazant and O. D. Velev, Phys. Rev. Lett., 2008, 100, 058302.

[4] F. Kogler and S. H. L. Klapp, EPL, 2015, 110, 10004.

[5] F. Guzman-Lastra, A. Kaiser and H. Löwen, Nat. Commun., 2016, 7, 13519.

[6] G.-J. Liao, C. K. Hall, and S. H. L. Klapp, Soft Matter, 2020, 16, 2208.

[7] G.-J. Liao, S. H. L. Klapp, Soft Matter, 2021, 17, 6833.

[8] H. Reinken, S. H. L. Klapp, M. Bär, and S. Heidenreich, 2018, Phys. Rev. E 97, 022613.

Magnetic Behavior Studies of Cobalt Ferrite Nanoparticles in Physiological Acceptable Concentrations

N. Lucht[1], R. P. Friedrich[2], S. Draack[3], C. Alexiou[2], F. Ludwig[3], B. Hankiewicz[1]

[1] *Institute of Physical Chemistry, University of Hamburg, Grindelallee 117, 20146 Hamburg*
[2] *Section for Experimental Oncology and Nanomedicine, University Hospital Erlangen, Glückstraße 10a, 91054 Erlangen*
[3] *Institute for Electrical Measurement and Principles of Electrical Engineering, Technical University of Braunschweig, Hans-Sommer-Straße 66, 38106 Braunschweig*

Medical applications for nanoparticles have been extensively discussed in the recent years. Nanoparticles offer a wide variety of potential applications in the medical field. Up to date there is much controversy regarding the toxicity of nanoparticles. In this work we present hard magnetic cobalt ferrite nanoparticles that show very low toxicity prima facie. These particles were then tested for their heating behavior in nontoxic concentrations.[1]

The cobalt ferrite nanoparticles are synthesized in a one-step coprecipitation and stabilized with sodium citrate. The particles can be additionally coated with a dense silica layer that provides chemical resistance and enables further functionalization. An embedding through a grafting to radical polymerization in a soft thermoresponsive polymer shell could be the next step for another application but was
skipped for this study as the particles need to be in a low viscous solvent for the conceived application. Inducing phase transitions in thermoresponsive matrices with hyperthermia is a very interesting topic by itself and will be examined in a later state of the project.

Preliminary toxicological data of the particle system shows little to no toxicity in the first 24 hours (Fig 1l). After 48 hours the particle system shows no toxicity in reasonable concentrations up to over 100 µg/mL while preserving a good magnetic moment (Fig 1m). The particles additionally express pure Brownian relaxation which is an excellent feature for fundamental research (Fig 1r). From a practical perspective there is a variety of potential applications. We built a custom hyperthermia coil to access the loss power of our particle samples in correlation with the toxicologic data. The loss power shows promising numbers. To calculate the loss power of a system there are generally two approaches: a calorimetric approach where the actual heating of a solvent is observed and an intrinsic approach where the possible power dissipation from a magnetic system is calculated.

The most common approach is the calorimetric in which the linear regime of a heating vs. time curve (compare Figure 2l) is

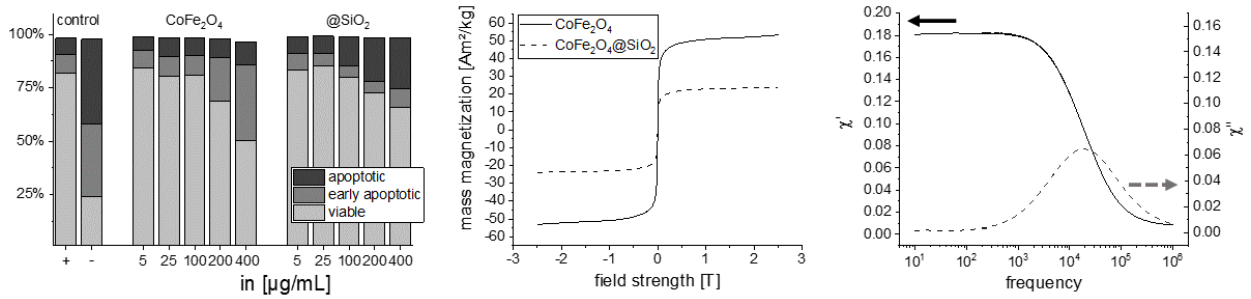

Figure 1. (l) Concentration series of Jurkat cell toxicity assay after 48 h comparing pristine $CoFe_2O_4$ particles with $CoFe_2O_4$@SiO_2 core-shell particles. (m) Mass normalized static magnetization curves measured via VSM of the two particle systems. (r) AC-susceptibility measurement of the pristine $CoFe_2O_4$ particles showing Brownian dominated relaxation.

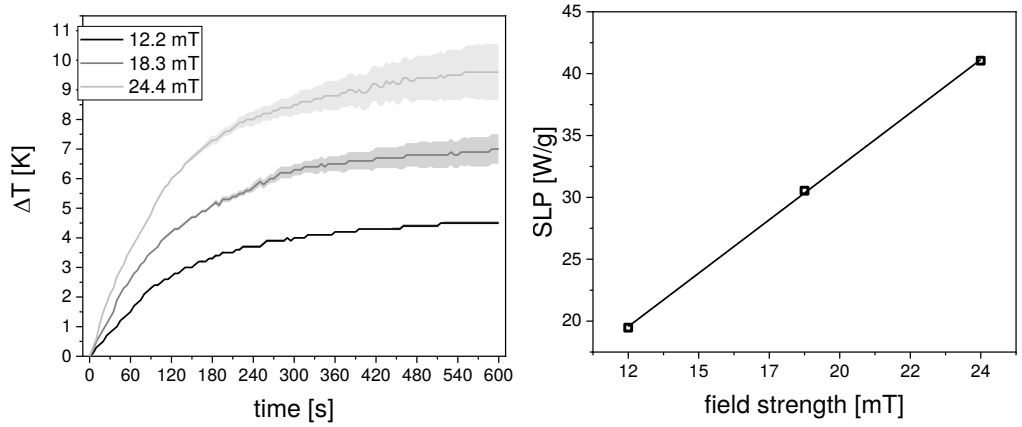

Figure 2. (l) time dependent heating behavior of 1 mL (10 mg/mL) citrate stabilized $CoFe_2O_4$ in water at differing field strengths. The error margins are depicted as clouds around the measured values and derive from coil heating. (r) Calculated SLP values as a function of the field strength.

used to calculate the specific loss power utilizing Eq. 1:

$$SLP\ [W * g^{-1}] = \frac{C}{m}\frac{\Delta T}{\Delta t} \quad (1)$$

with the heat capacity of the solvent C, the particle mass used. The main advantage of this approach is the easy to access measurement variables being temperature and time. This is also our favored approach. The intrinsic approach takes the actual magnetic system into account following Eq. 2:

$$ILP\ [W * g^{-1}] = \frac{1}{m}\pi\mu_0\chi'' f\ \frac{B^2}{\mu^2} \quad (2)$$

This approach utilizes both intrinsic particle parameters as the AC-susceptibility χ, the magnetic permeability μ and of course the particle mass used. Additionally, the field parameters, i.e. the field strength B and the field frequency f, are considered. While this equation delivers very exact results it has the inherent disadvantage that the magnetic permeability is not easy to access and no table value as it vastly discriminates comparing different particle systems which is the reason why only Eq. 1 was used to calculate the SLP in Figure 2. It is planned to access the ILP in the future to see if comparable results can be created though.

We have established a stable hard magnetic system with low short-term toxicity and a comparably high magnetic moment. We could assess the specific loss power of our system and reach reasonable values for a potential application in magnetic hyperthermia. The particle system will be tuned to further decrease their toxicity while maintaining the same magnetic properties. We would also like to access the actual permeability of our particle system and compare ILP and SLP.

Acknowledgments

DFG is kindly acknowledged for funding this project via the SPP1681 (grant number: FI-1235/2-2).

References

[1] Lucht, N.; Friedrich, R.P.; Draack, S.; Alexiou, C.; Viereck, T.; Ludwig, F.; Hankiewicz,B. Biophysical Characterization of (Silica-coated) Cobalt Ferrite Nanoparticles for Hyperthermia Treatment *Nanomaterials* 2019, 9, 1713-1726.

Studies about the Design of Magnetic Bionanocomposite

R. Müller[1], T. Heinze[2]

[1] *Leibniz-Institute of Photonic Technology (IPHT), P.O.B. 100239, D-07702 Jena, Germany*
[2] *Institute of Organic Chemistry and Macromolecular Chemistry, Friedrich Schiller University of Jena, Humboldt-straße 10, D-07743 Jena, Germany*

The contribution gives an overview about the work on meltable magnetic bionanocomposite in the frame of the SPP1681.
Magnetic nanocomposites are a class of smart materials that have attracted recent interest as drug delivery systems or as medical implants. A new approach toward the biocompatible nanocomposites suitable for remote melting is presented. It is shown that magnetite nanoparticles (MNP) can be embedded into a matrix of biocompatible thermoplastic dextran esters. For that purpose, fatty acid esters of dextran with adjustable melting points in the range of 30 − 140 °C were synthesized via esterification of the polysaccharide by activation of the acid as iminium chlorides [1]. A method for the preparation of magnetically responsive bionanocomposites (BNC) was developed consisting of combined dissolution/suspension of the dextran ester and hydrophobized MNPs in an organic solvent followed by homogenization, casting of the solution, drying, and melting of the composite for a defined shaping [2]. This process leads to a uniform distribution of MNPs in BNC as revealed by scanning electron microscope (SEM). Samples of different geometries were exposed to high frequency alternating magnetic field (AMF). It could be shown that defined remote melting of such biocompatible nanocomposites is possible for the first time [3]. This may lead to a new class of magnetic remote-control systems, which are suitable for controlled release applications. Release experiments were carried out using Rhodamine B (RhB) or green fluorescent protein (GFP) as model drugs under the influence of a high frequent AMF (20 kA/m at 400 kHz) to evaluate their potential use as drug delivery system and showed that on-demand release is realized applying the external AMF [4]. The BNC possessed a long-term stability (28 d) of the incorporated iron oxide particles after incubation in artificial body fluids. Temperature dependent mobility investigations of MNP in the molten BNC were carried out by optical microscopy, magnetometry, and alternating current (AC) susceptibility and Mössbauer spectroscopy measurements at the University of Duisburg-Essen [5]. Optical microscopy shows a movement of agglomerates and texturing in the micrometer scale, whereas AC-susceptometry and Mössbauer spectroscopy investigations reveal that the particles perform diffusive Brownian motion in the liquid polymer melt as separated particles rather than as large agglomerates. Furthermore, a texturing of MNP in the polymer matrix by a static magnetic field gradient was investigated [6]. Cross-linking of cross-linkable dextran esters after irradiation of the BNC prevents a melting that can be used to influence texturing procedures. A movement of MNPs could be observed only in the area of the composite layer that was not exposed to UV light. First analogous experiments with local irradiation through an optical mask show a concentration of MNPs along the mask structure and a partly texturing in different areas of the composite layer.

Acknowledgments

The financial support of the German Science Foundation (DFG, priority program SPP 1681, contracts HE2054/14-1, HE2054/14-2, HE2054/22-1, MU2382/4-1, MU2382/4-2 and MU2382/5-1) is acknowledged.

The authors are very thankful to former coworkers in the project: Dr. M. Zhou, Dr. N. Kuhl, J. Kuchinka and A. Dellith.
We thank our SPP partners in AG Dutz (TU Ilmenau) for providing MNPs and AG Wende (University Duisburg-Essen) for ACS and Mössbauer measurements, AG Odenbach (TU Dresden) for rheological measurements, AG Clement (University Hospital, Jena) for cell experiments for biocompatibility studies, Prof. D. Fischer and coworkers (University Jena, no SPP member) for investigations on the biodegradation of the bionanocomposites in artificial body fluids, as well as all the colleagues of the priority program SPP 1681 for useful discussions.

References

[1] T. Liebert, J. Wotschadlo, P. Laudeley, T. Heinze, Meltable Dextran Esters as Biocompatible and Functional Coating Materials. Biomacromolecules 2011, 12 (8), 3107–3113.
[2] M. Zhou, T. Liebert, R. Müller, A. Dellith, C. Gräfe, J. H. Clement, T. Heinze, Biomacromolecules 2015, 16, 2308-2315.
[3] R. Müller, M. Zhou, A. Dellith, T. Liebert, T. Heinze, Meltable magnetic biocomposites for controlled release, J. Magn. Magn. Mater. 431 (2017) 289–293
[4] T. Heinze, R. Müller, M. Zhou, M. Rabel, P. Warncke, D. Fischer, Studies on the Controlled Release of Drugs from Magnetic Nanobiocomposites, Indones. J. Fundam. Appl. Chem., 4(1), 2019, 1-8
[5] R. Müller, M. Zhou, T. Liebert, J. Landers, S. Salamon, S. Webers, A. Dellith, D. Borin, T. Heinze, H. Wende, Mobility Investigations of Magnetic Nanoparticles in Biocomposites. Mater. Chem. Phys. 2017, 193, 364–370.
[6] R. Müller, J. Kuchinka and T. Heinze, Studies about the design of magnetic bionanocomposite, Phys. Sci. Reviews, doi.org/10.1515/psr-2019-0122

Particle jumps in chains and lattices of magnetic particles

H. Schmidt[1], G. K. Auernhammer[2]

[1]*Max Planck Institute for Polymer Research, Ackermannweg 10, 55128 Mainz, Germany*
[2]*Leibniz Institute of Polymer Research, Hohe Straße 6, 01069 Dresden, Germany,*
Email: auernhammer@ipfdd.de

We investigate the behavior of nickel particle embedded in an elastic matrix under the influence of the applied magnetic fields. These particle show a very small magnetization of the particles at zero field. For high magneto-mechanical effects, we typically use particle diameters in the range of 100 µm to 200 µm. Long (non-contacting) particle chains or laterally extended (non-contacting) particle arrangement are prepared in an (essentially) elastic PDMS gel matrix.
Under the action of an applied magnetic field two mechanisms have to be balanced: The magnetic attraction between the particles and the elastic force by the matrix that opposes any relative motion of the embedded particles. In systems with two or three particles, this leads to sudden jumps into contact of particles, e.g., under rotation of the magnetic field. For extended particle chains, the balance between the magnetic attraction and the elastic hinderance leads to the formation of contacting groups of particles, Fig. 1. These groups of particles have some similarities to longitudinal waves [1] along the chain.
In laterally extended arrangements of particles, the situation is more complex. The basic balance between magnetic attraction and elastic hinderance stays unchanged, Fig. 2. However, the degrees of freedom increase significantly. The groups that form depend i) on the initial distance of the particles, ii) the particle-particle distances of the surrounding particles, and iii) the magnetic field history. We dis-

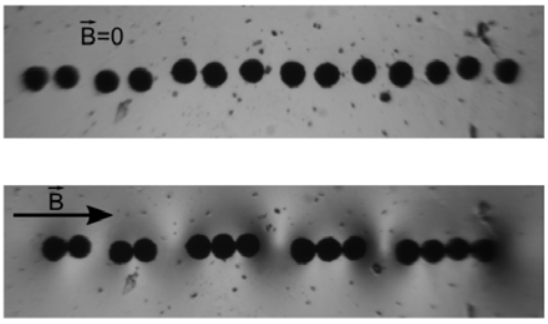

Figure 1: Group formation of magnetic particles from an initial chain of non-contacting particles.

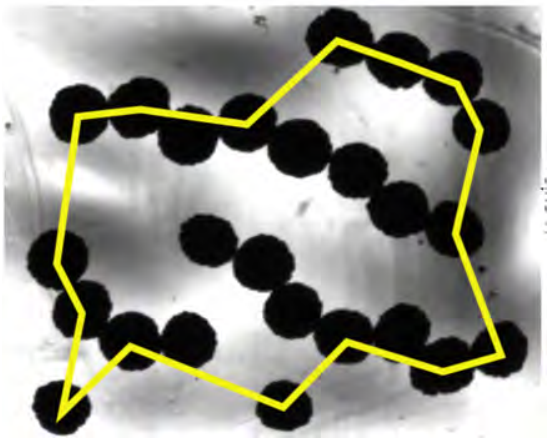

Figure 2: Group formation of magnetic particles from a laterally extended arrangement of non-contacting particles under applied magnetic field. The particles at the border of the initial (field-free) arrangement are marked.

cuss these effects using lattice like arrangements of nickel particles under rotating magnetic fields. The macroscopic shape change turns out to be a complex function of these effects.

Acknowledgments

Funded by the German Research Federation (DFG) within the SPP1681 Grant AU321/3.

References

[1] H. Schmidt, B. B. Straub, D. Sindersberger, U. Bröckel, G. J. Monkman, and G. K. Auernhammer. Collision and separation of nickel particles embedded in a polydimethylsiloxan matrix under a rotating magnetic field: A strong magneto active function. *Colloid and Polymer Science*, 299:955–967, 2021.

X-ray microtomography investigation of NdFeB-particle motion in magnetorheological elastomers

M. Schümann, S. Odenbach

Technische Universität Dresden, 01069 Dresden, Germany

Magnetorheological elastomers are a class of smart hybrid material where magnetic microparticles are embedded in an elastomer matrix. The combination of elastic and magnetic properties leads to a highly complex material behaviour, which is strongly affected by the arrangement and the magnetically induced motion of the magnetic particles. Thus, the knowledge of the internal particle structure is a key to gain a deeper understanding of the complex material behaviour. In the last few years magnetorheological elastomers utilizing magnetically hard particles gained central interest in research. The ability to magnetize the particles remanently adds further functionality to this material using passive tuning and active control, as well as arouse interest for different applications of those materials [1,2]. A number of recent works are devoted to theoretical and experimental studies of macroscopic magnetic properties of magnetorheological elastomers containing magnetically hard particles [3,4]. Despite the good qualitative agreement of experimental and theoretical results, quantitative deviations regarding the results can be significant. This is also due to the lack of information about the real particle microstructure and its changes during the magnetization of the material. This issue emphasizes the need of profound and accurate data regarding the particle microstructure. The linking of experimental results regarding microscopic phenomena and overall macroscopic material behaviour would give a scale bridging description, which is crucial for achieving a comprehensive understanding of the material behaviour. This linking can only be achieved with a likewise comprehensive set of measurements applied to one single sample material.

The current study presents a comprehensive investigation on the NdFeB-particle structure in an elastic matrix influenced by magnetic fields and covers the whole transition from an isotropic particle distribution to particle chains. With these results a direct linking from structural properties to mechanical behaviour made possible.

Figure 1. 3D-model obtained from the reconstructed X-ray microtomography data showing a detailed view of the same few particles, captured at different magnetizations steps. From left to right: B_{ext}= 0, B_{ext}= 1250 mT and B_{ext}= 2000 mT.

The utilized matrix material features fully elastic properties, providing fully reversible deformation behaviour with embedded particles. A stepwise magnetization of the material was used and the X-ray microtomography was applied to analyze the internal particle structure. Prior to microstructural investigations, composite samples were magneto-mechanically and magnetically characterized. The collected tomography data of the particle structure was evaluated on a single particle basis as well as by means of a direction dependent pair correlation function (PCF). The remanently magnetizable particles introduce non-reversible properties. Figure 1 shows a small excerpt of tracked particles along increasing external magnetization B_{ext}. After magnetization at B_{ext} = 1000 mT the material exhibits a magnetorheological effect, which increases for

higher magnetizations. By the evaluation of the captured X-ray microtomography data it was shown, that a strong rotation of the particles is observable in presence of a field with B_{loc} = 250 mT, if the sample was magnetized before using B_{ext}. This strong rotation is a mostly reversible behaviour, as if the field is removed, the particles rotate back. The remaining rotation induced by the magnetization at 2000 mT is minor. The conducted particle tracking proved to be a powerful and sensitive tool to evaluate the rotational behaviour of the particles in further detail.

The translation of the particles, which results in a transition from the observed initial isotropic spatial particle distribution to particle chains, was found to be an irreversible process. The results obtained by the particle tracking were found to be sensitive to the image registration. Thus, the evaluation of the particle translation by means of direction dependent PCF proved to be the more suitable approach. Nevertheless, trajectories from individual particles as obtained by the particle tracking can act as input data for future theoretical modelling or simulation of those materials.

The evaluation of the direction dependent PCF verified the characteristic transition point at B_{ext} = 1000 mT. After this magnetization step, a transition to an anisotropic particle distribution was verified, indicating a commencing non-reversible chain formation process. The development of anisotropy, quantitatively described by the maximum value of the PCF in *z*-direction (direction of B_{loc} and B_{ext} fields), clearly corresponds to the results regarding the magnetorheological effect R_E obtained within magneto-mechanical characterization of the composite under study (Figure 2). The parameter R_E was calculated from the Young's moduli E_B, measured at B_{loc}=250 mT, and E_0 measured at B_{loc}=0 as $R_E = \frac{E_B - E_0}{E_B}$. The measurements were performed with one single sample undergoing exactly the same magnetic situations as the sample utilized for tomography. The correlation of distinct changes in particle microstructure and magnetically affected macroscopic mechanical properties provides a scale bridging link and thus an important contribution in gaining a deeper understanding of the complex material behaviour of magnetorheological elastomers. In close connection with theoretical modelling and simulation approaches, those scale bridging links will provide the most promising experimental data, to enable a targeted tailoring of magnetorheological elastomers to fit their desired properties for future technical applications.

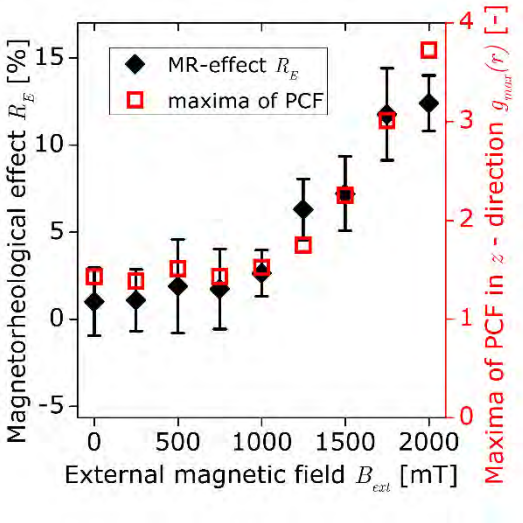

Figure 2. Peak values of the PCF data regarding z-direction for every magnetization step plotted together with the data of the magnetorheological effect.

Acknowledgments

Financial support by Deutsche Forschungsgemeinschaft (DFG) under Grant Od 18/21 within the priority program SPP1681 is gratefully acknowledged.

References

[1] D. Borin, G. Stepanov, E. Dohmen, Archive of Applied Mechanics 89 (2019) 105-117

[2] T. Becker, K. Zimmermann, D. Borin, G. Stepanov, P. Storozhenko, J. Magn. Magn. Mater. 449 (2018) 77-82

[3] M Vaganov, D. Borin, S. Odenbach, Y. Raikher, J. Magn. Magn. Mater. 459 (2018) 92-97

[4] M Vaganov, D. Borin, S. Odenbach, Y. Raikher, Physica B: Cond. Matter 578 (2020) 411866

Magneto-mechanical coupling of single domain particles in soft matter systems

J. Seifert,[1] K. Koch,[1] M. Hess,[1] A. M. Schmidt[1]

[1] *Institut für Physikalische Chemie, Universität zu Köln*

Combining inorganic magnetic particles with complex soft matrices such as liquid crystals, biological fluids, gels, or elastomers, allows access to a plethora of magnetoactive effects that are useful for sensing and actuation perspectives, allowing inter alia to explore and manipulate material properties on the nanoscale. Our works in the SPP1681 contribute to the recent advancement on employing magnetic nanoparticles either as tracers for dynamic processes, or as nanoscopic actuating units. Therefore, the design of hybrid materials that can be manipulated by magnetic fields is possible by incorporating inorganic magnetic nanoobjects into complex soft matrices such as gels, elastomers, liquid crystals, or biological fluids in a predetermined way. By variation of the particle characteristics in terms of size, shape, surface functionality and magnetic behaviour, the interaction between the probe or actuator particles and their environment can be systematically tailored in wide ranges, giving insight into the relevant structure-property relationships.

Magnetic Particle Nanorheology

The original idea of particle-based microrheology is to analyze the rheological results of small samples in a non-destructive way. However, if the probe size gets more similar to the relevant length scales of the matrix material, the pathway to the investigation of size dependent properties is opened, as it is relevant for internal dynamics in systems such as nanocomposites and cells.

The strongly size dependent properties that are measured in nanorheological experiments on microstructured samples make this method a promising candidate for the development of a method capable of determining local rheological properties on a nanoscale. The use of magnetically blocked, nanoscopic particles as tracers under the influence of an oscillating magnetic field is a particularly promising approach. The response of the particles in terms of their magnetic susceptibility is recorded, and in analogy to classical macrorheology, the phase shift of the response signal delivers information on the complex susceptibility and thus on the frequency-dependent excitation of the particle rotation.

By employing magnetically blocked nanoparticles as nanoscopic, quasi-dipolar magnetic probes, the complex dynamic behavior of soft matter at the particle scale is investigated in fluid media of increasing complexity. This approach allows the extraction of the complex, frequency-dependent rheological information from AC-susceptibility measurements of tracer particles and polymer solutions.

MP as tracers and actuators in nanostructured solids

The combination of MP and elastic, polymeric matrices leads to magnetosensitive hybrid materials.

The architecture with the strongest interactions between MP and polymer chains is represented by particle-crosslinked ferrohydrogels and -elastomers. This type of stimuli responsive material gives rise to improved material properties due to a strong magneto-mechanical coupling and a novel response mechanism to an external magnetic field. A simple effect of the cova-

lent attachment is that in contact with swelling media no particle loss is observed due to diffusion, and the materials may therefore be used over many cycles even in contact with biological tissue. If the network is solely crosslinked by the magnetic nanoparticles, strongly particle content depending properties are obtained. As particle component, either spherical particles also anisotropic particles, e. g. spindle-type hematite particles can be used.

Magnetically doped liquid crystals

Liquid crystal (LC) based magnetic materials consisting of LC hosts doped with functional magnetic nanoparticles enable optical switching of the mesogens at moderate magnetic field strengths and thereby open the pathway for the design of novel smart devices. A promising route for the fabrication of stable ferronematic phases is the attachment of a covalently bound LC polymer shell onto the surface of nanoparticles. With this approach, ferronematic phases based on magnetically blocked particles and the commercial LC 4-cyano-4'-pentylbiphenyl (5CB) liquid crystal were shown to have a sufficient magnetic sensitivity, but the mechanism of the magneto-nematic coupling is unidentified. To get deeper insight into the coupling modes present in these systems, we prepared ferronematic materials based on superparamagnetic particles, which respond to external fields with internal magnetic realignment instead of mechanical rotation. This aims at clarifying whether the hard coupling of the magnetization to the particle's orientation (magnetic blocking) is a necessary component of the magnetization-nematic director coupling mechanism. We herein report the fabrication of a ferronematic phase consisting of surface-functionalized superparamagnetic Fe_3O_4 particles and 5CB. We characterize the phase behavior and investigate the magneto-optical properties of the new ferronematic phase and compare it to the ferronematic system containing magnetically blocked $CoFe_2O_4$ particles to get information about the origin of the magneto-nematic coupling.

The incorporation of magnetic nanoparticles into various structures is thus a versatile approach to find access to the rich world of magnetically responsive materials. Key to understanding and optimizing the composite systems is a detailed knowledge of the underlying particle-matrix interactions in such hybrid materials. These interactions are based on the surface chemistry of the particles and their coupling to the surrounding matrix, but also fundamentally depend on the relative size of the particles to characteristic sizes in the matrix, such as mesh size or correlation length. In combination with elastic matrices, the mutual interaction of particle and matrix can be used to gain more insight in the coupling behavior, or information about the properties of the elastic and magnetic component. While all these investigations demonstrate the utility of magnetically responsive hybrid materials, many open questions still remain on the coupling of MP and complex matrices and on the applicability of these responsive materials.

Acknowledgments

This work was funded in the priority programm DFG-SPP 1681 under grant no. SCHM1747/10.

References

J. Seifert, K. Koch, M. Hess, A. M. Schmidt, „Magneto-mechanical coupling of single-domain particles in soft matter systems“ Phys. Rev. Sci., 2020.

Rheological behavior of magnetic hydrogels

L. Selzer, S. Odenbach

Technische Universität Dresden, Institute of Mechatronic Engineering, D-01062 Dresden, Germany

Introduction

Hydrogels are polymeric soft materials which have gained increased interested since the 1970s and are widely used in today's everyday life as contact lenses and superabsorbers. Depending on the monomers used, they can intrinsically be sensitive to temperature, pH or salt concentration, making them suitable as sensor and actuator materials. By adding magnetic particles, they can be further functionalized to interact with magnetic fields. We investigated the rheological behavior of a temperature sensitive gel with magnetic particles at different degrees of swelling.

Materials and Methods

A magnetic hybrid material was synthesized by mixing magnetite particles with a N-isopropylacrylamide and laponite solution, which was polymerized using tetramethylethylenediamine and sodium persulfate as catalyst and initiator. With a Haake MARS III with a custom-made magnetic cell, we measured step response of the shear moduli to different magnetic field strengths up to 500 kA/m using oscillatory testing in the linear viscoelastic region of the samples. This was carried out in the swollen state at 20 °C and the deswollen state of the gel at 40 °C for particle contents ranging from 10 to 60 wt%. Samples were stored at 20 °C and 40 °C till a swelling equilibrium was reached before any measurement. The magnetorheological effect (*MR-effect*) was derived as a factor for net increase by a fit function using (1) and (2) which compensated for baseline drifts (*BLD*), which especially occurred at 40 °C. As seen in **Fehler! Verweisquelle konnte nicht gefunden werden.**, only data of the timeframes A (before magnetic field), M (during the magnetic field) and E (after the magnetic field) were used to fit steady state behavior and ignore dynamic effects.

$$G_0 = BLD \cdot t \quad (1)$$

$$G = G_0 \cdot (1 + MR\text{-}effect) \quad (2)$$

Results

Increasing the particle content did not lead to significant changes of the swelling behavior or the shear moduli when no magnetic field was applied. When a magnetic field was applied the samples showed an increasing MR-effect with increasing particle content up to a factor of 1.5 in the swollen state. The effect showed saturation behavior for all particle contents at higher field strengths. In the deswollen state the shear moduli increased by approximately two ordors of magnitudes compared to the swollen state, while the maximum MR-effect observed was 0.5. Changes to storage and loss modulus from swelling behavior or MR-effect were largely the same.

Discussion

Because hydrogels consist of over 70% water even with a high particle content of 60 wt% in the deswollen state, particles do not seem to have an influence on the shear moduli when no fields were applied. Changes to the shear moduli from the swelling and deswelling behavior of the hydrogels are orders of magnitude larger than the observed MR-effect. By deswelling two different effects occur which are influencing the MR-effect. On the one hand the particle volume concentration increases by deswelling, which would lead to an increase of the

MR-effect, since more magnetic material is available per volume.

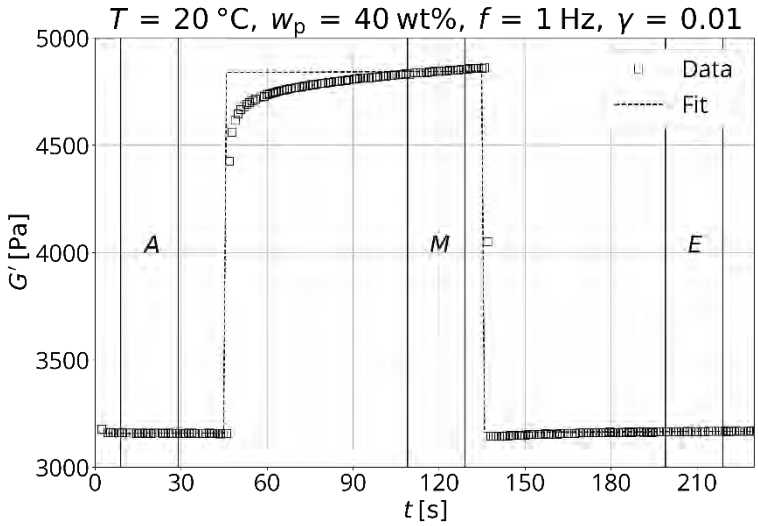

Figure 1. Step response of the storage modulus of a sample with a 40 wt% particle content at 20°C and a field strength of 500 kA/m.

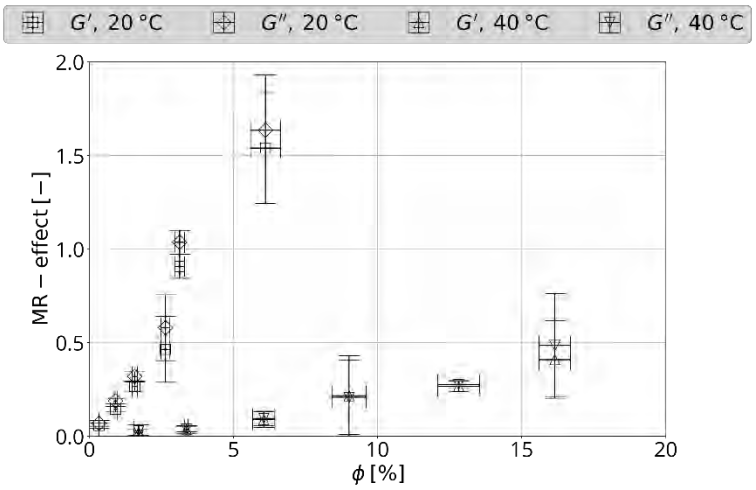

Figure 2. MR-effect over volume concentration of particles.

On the other hand, the baseline of moduli increases by orders of magnitude, limiting the particle mobility inside the matrix and thus the orientation of particles and formation of chains, which are linked to MR-effects. [1] Since the MR-effect decreases by deswelling, the mobility decrease is the dominant effect. This is best seen in Figure 2, where 60 wt% at 20 °C and 30 wt% at 40 °C have the same volume concentration of $\phi = 6$ %, but have MR-effects of 1.5 and 0.1 respectively.

Acknowledgments

The work presented in this article was funded by the German Research Foundation within the framework of the Research Training Group 1865 “Hydrogel-based Microsystems”.

References

[1] Schümann, M, D Yu Borin, J Morich, and S Odenbach. “Reversible and Non-Reversible Motion of NdFeB-Particles in Magnetorheological Elastomers.” *Journal of Intelligent Material Systems and Structures* 32, no. 1 (January 2021): 3–15.

Synthesis and Characterization of Citrate-Stabilized Gold-Coated SPIONs for Biomedical Applications

R. Stein[1], B. Friedrich[1], M. Mühlberger[1], N. Cebulla[1], E. Schreiber[1], R. Tietze[1], I. Cicha[1], C. Alexiou[1], S. Dutz[2], A. R. Boccaccini[3], H. Unterweger[1]

[1] *Department of Otorhinolaryngology-Head and Neck Surgery, Section of Experimental Oncology and Nanomedicine (SEON), Else Kröner-Fresenius-Stiftung-Professorship, Universitätsklinikum, Erlangen, Germany*
[2] *Institute of Biomedical Engineering and Informatics, Technische Universität Ilmenau, Ilmenau, Germany*
[3] *Institute of Biomaterials, University of Erlangen-Nuremberg, Erlangen, Germany*

Gold-coated and surface functionalized superparamagnetic iron oxide nanoparticles (Au-SPIONs) have great potential for future application in various biomedical applications. In this study [1], a novel SPION system with thiol-binding capability was presented as a basic delivery system for various medical applications, such as intravascular drug delivery or photothermal therapy. Gold-coated SPIONs were prepared by precipitating gold salt onto citrate-stabilized SPIONs (Cit-SPIONs) according to a modified method of Elbialy et al [2] for the synthesis of gold nanoparticles, and the stabilization was further increased by adding additional citrate. The focus of this work was to systematically explore the effects of various synthesis parameters, such as citrate stabilization, reaction time, reaction temperature, precursor concentration, and gold concentration, on the particle properties of the prepared nanoparticles to produce a reproducible and controllable nanosystem.

To demonstrate the functionalization capability of the particles for various medical applications, a thiol group containing the amino acid L-cysteine was attached to the citrate-stabilized gold surface. Compared to pure Cit-SPIONs, a significantly higher binding of thiol-containing L-cysteine to the particle surface was observed (7% vs 53%). However, the surface binding of large thiol-containing molecules and the binding capacity of e.g. drugs to Cit-Au-SPIONs remains to be confirmed in future studies.

The synthesized particles were first investigated physico-chemically. On scanning electron microscopy (SEM) images, Cit-Au-SPION clusters (Fig. 1c) resembled the spherical clusters seen in pure Cit-SPIONs (Fig. 1a), whereas non-stabilized Au-SPIONs form large irregularly shaped structures (Figure 1b). Accordingly, dynamic light scattering (DLS) data (Fig. 1d) demonstrated a large increase in the Z-average from 107 ±3 nm with a corresponding polydispersity index (PDI) of 0.15 ±0.03 in pure Cit-SPIONs to 405 ±83 nm with a corresponding PDI of 0.25 ±0.06 in non-stabilized Au-SPIONs. The presence of additional citrate ions on Cit-Au-SPIONs reduced the Z-average to 152 ±5 nm with a corresponding PDI of 0.19 ±0.01, improved the reproducibility in size of different particle batches and enhanced the long-term stability during storage. Hence, the gold coating, which were confirmed by X-ray diffraction measurements, resulted in stable Z-means, improved long-term dispersion stability, and moderate dispersion pH values. To exclude the possibility of simultaneous formation of pure gold nanoparticles without any attachment to SPIONs, a magnet was placed next to Au-SPION and Cit-Au-SPION dispersions. After 8h, the supernatants of both samples were colorless, indicating that all nanosized gold was attached to SPIONs. Both, Cit-SPIONs and Cit-Au-SPIONs, exhibited superparamagnetic behavior and the H_C values were 0.221 kA/m for Cit-SPIONs and 0.225 kA/m for Cit-Au-SPIONs. However, the Cit-Au SPIONs showed reduced saturation magnetization by 40.7% compared to pure citrate coated SPIONs (Fig. 1e). Further studies will

evaluate the magnetic attraction of the SPIONs to the target tissue and enhance cellular particle uptake if necessary.

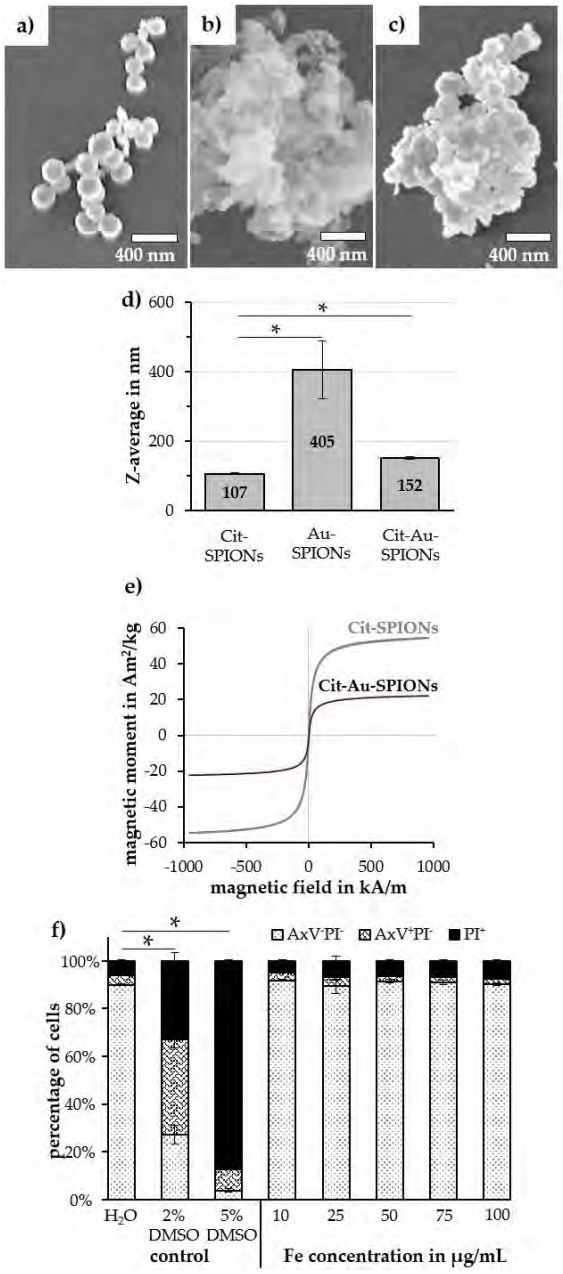

Figure 1. Particle characterization. (**a**) Scanning electron microscopy (SEM) images of pure Cit-SPION clusters, (**b**) Au-SPION clusters and (**c**) Cit-Au-SPION clusters. (**d**) Mean Z-averages over 21 days for Cit-SPIONs, Au-SPIONs and Cit-Au-SPIONs. (**e**) Magnetization curves of Cit-SPIONs and Cit-Au-SPIONs. (**f**) Jurkat cell viability evaluated by Annexin A5 fluorescein isothiocyanate (FITC) conjugate (AxV)/propidium iodide (PI) staining after 48 h of incubation with different Cit-Au-SPION concentrations. Viable cells are indicated as AxV−PI−, early apoptotic cells as AxV+PI− and late apoptotic or necrotic cells as PI+.

Finally, Jurkat cell viability were determined by Annexin A5 fluorescein isothiocyanate (AxV)/propidium iodide (PI) staining and measured by flow cytometry (Fig. 1f) [3]. Sterile Cit-Au SPIONs showed no significant effect on Jurkat cells at concentrations up to 100 µg Fe/mL for 48 h, although Lucifer Yellow staining demonstrated significant particle uptake already after 24 h. Further haemocompatibility studies will follow to ensure that the particles have no adverse effects on blood and blood components.

In summary, low cytotoxicity in Jurkat cells, the promising physicochemical characteristics and enhanced accumulation of thiol-containing L-cysteine indicate a high potential of Cit-Au-SPIONs for future medical applications.

Acknowledgments

This work was funded in part by the Deutsche Forschungsgemeinschaft (German Research Foundation; CI 162/2-3).
The authors thank the Manfred-Roth-Stiftung, Fürth, Germany and the Forschungsstiftung Medizin am Universitätsklinikum Erlangen, Erlangen, Germany for the support.

References

[1] R. Stein, B. Friedrich, M. Muhlberger, N. Cebulla, E. Schreiber, R. Tietze, I. Cicha, C. Alexiou, S. Dutz, A.R. Boccaccini, H. Unterweger, Synthesis and Characterization of Citrate-Stabilized Gold-Coated Superparamagnetic Iron Oxide Nanoparticles for Biomedical Applications, Molecules 25(19) (2020).
[2] N.S. Elbialy, M.M. Fathy, W.M. Khalil, Preparation and characterization of magnetic gold nanoparticles to be used as doxorubicin nanocarriers, Phys. Med. 30(7) (2014) 843-8.
[3] C. Janko, L. Munoz, R. Chaurio, C. Maueroder, C. Berens, K. Lauber, M. Herrmann, Navigation to the graveyard-induction of various pathways of necrosis and their classification by flow cytometry, Methods Mol. Biol. 1004 (2013) 3-15.

Magnetic Hybrid Elastomers: magnetic response and elastic anisotropy

G.V. Stepanov[1], D.Yu. Borin[2], A.V. Bakhtiiarov[1], E.Yu.Kramarenko[3], P.A. Storozhenko[1]

[1] *State Research Institute for Chemical Technologies of Organoelement Compounds 111123, Moscow, Russia*
[2] *Institute of Mechatronic Engineering, TU Dresden, 01062 Dresden, Germany*
[3] *Faculty of Physics, Moscow State University, Moscow, 119991 Russia*

Hybrid magnetic elastomers (HME) have been intensively studied as materials prospective for designing field-controllable damping devices and acceleration sensors. Among their components, they contain magnetically hard and magnetically soft fillers dispersed in a polymer matrix. The behavior of HME placed in a magnetic field appears to be different from that exhibited by 'classic' magnetorheological elastomers. Their specific features are determined by the presence of magnetically hard components [1-4]. Influenced by a magnetic field, the material gets magnetized which results in internal structuring and rotation of magnetic filler particles [5-7]. The intensity of these processes is determined by the magnetic properties of the filler, strength of the external field, and elasticity of the polymer matrix. Such hybrid elastomers have been used for designing acceleration sensors [8-9]. The main amount of time jointly spent on the experimental work by our research teams has been dedicated to investigation of the rotation of magnetically hard particles contained in the polymer matrix [10-19] and modelling of processes of this type.

Magnetic response

Figure 1 is a demonstration of the different behavior of magnetic elastomer filled with magnetically hard particles and having a polymer matrix elasticity modulus of 300-400 kPa. The hysteresis loop of such a composite can exhibit a tendency to get wider as the external magnetic field amplitude increases (curve 1) as well as demonstrates a narrowing (curve 2). This effect can be explained by the beginning of rotation of the magnetic particles. Magnetized to a sufficiently high degree, the particles tend to make their magnetic moments co-linear with the direction of a reverse magnetic field. As a result, a certain amount of particles has it done not by changing the direction of their moments to opposite internally but by turning inside the polymer themselves. This phenomenon is well seen from a set magnetization curves recorded with various magnetic field amplitudes [5-6, 12,14]. Samples based on soft polymer matrices with elasticity moduli of 5-10 kPa filled with magnetically hard particles having a coercivity of 9 kOe demonstrate hysteresis loops intersecting the axis of abscissas close to the origin, as do magnetically soft materials (Fig. 2).

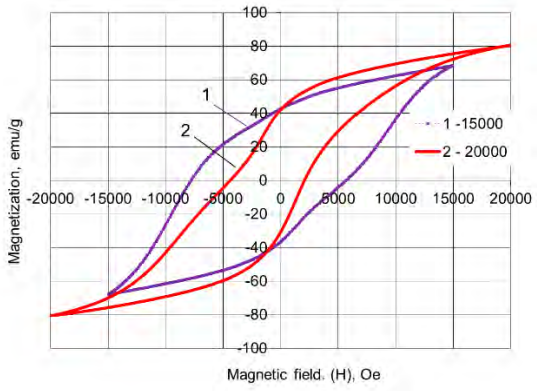

Figure 1. Hysteresis loops recorded for hybrid magnetic elastomer with field amplitudes of 15 kOe (1) and 20 kOe (2).

Taking values below 100 Oe, the observed 'coercivity' may even 'become negative' on the ascending branch. At the same time, as may be seen from Figure 2, the remanence also remains to be close to zero [12, 14]. This feature of the ascending curve is based on that the polymer matrix tends to place the

magnetic particles in their initial positions occupied by them on the initial magnetizing during sample polymerizing, turning back those of them which have remained turned over experiencing the action of a reverse field when the field is off (span 5-6 in Figure 2).

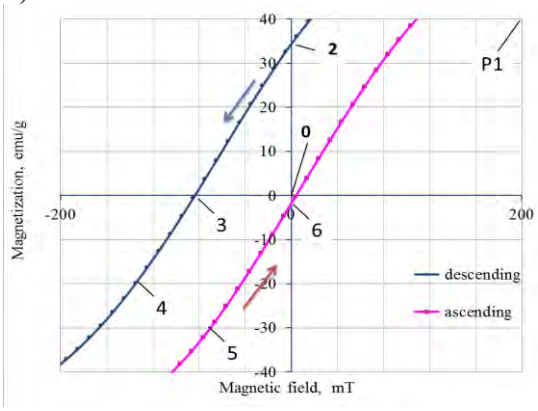

Figure 2. Middle part of the hysteresis loop demonstrated by hybrid magnetic elastomer with a soft matrix.

However, owing to their significant remanence, the particles demonstrate attraction to each other. Competition of the elastic forces and dipole interactions results in the formation of circular structures (points from 5 to 6 in Figure 2) [14]. The structuring processes are demonstrated in detail in the video http://www.magntolab.ru/video/video2_00.mp4.

Elastic anisotropy

If polymerized from liquid form under the influence of a magnetic field or subjected to its action before polymerizing, such an elastomer gains a certain anisotropy of elasticity (Fig. 3).

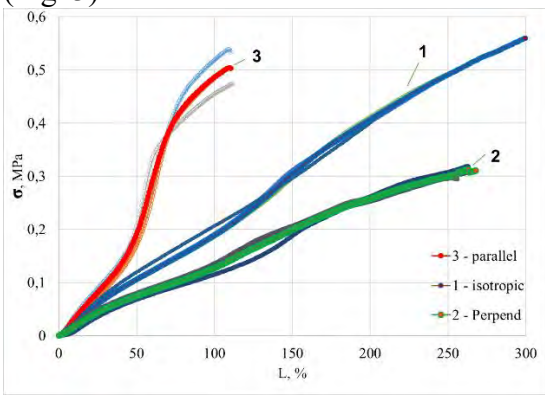

Fig. 3. Tension inside the sample being stretched. 1 – isotropic elastomer, 2 – stretching perpendicular to the anisotropy, 3 – stretching parallel to the anisotropy.

A sample of silicone resin-based elastomer with a concentration of plate-like carbonyl iron particles of 30 wt.% was polymerized after being placed in a field of 1 kOe. The strips cut out of it were of two types – the length perpendicular and parallel to the initial magnetic field direction, denoted by 2 and 3, respectively. The isotropic specimen (1) was fabricated without external field. As may be seen from Figure 3, the elasticity anisotropy equals 5, which means that the elasticity of a sample stretched along the direction of the initial field is higher by 5 times in comparison to that of a sample stretched in the direction perpendicular to the magnetization vector.

Acknowledgments

This work is supported by the (DFG) and the (RFBR) within the projects DFG Bo 3343/3-1 and RFBR 19-53-12039.

References

[1] G.V. Stepanov, A.V. Chertovich, E.Yu. Kramarenko, JMMM,324 (2012) 3448.
[2] D. Borin, G. Stepanov. J OPTOELECTRON ADV M. 15 (3-4) (2013) 249–253.
[3] Stepanov G.V., Borin D.Yu, Kramarenko E.Yu Polymer Sci, Ser. A,(56), 2014, No. 5, 603
[4] E Yu Kramarenko, A V Chertovich, G V Stepanov 2015 Smart Mater. Struct. 24
[5] G. Stepanov, D. Borin, P. Storozhenko, JMMM 431(2017)138–140.
[6] G. Stepanov, D. Borin, A. Bakhtiiarov, Smart Mater Struct 26 (2017) 035060.
[7] J. Linke, D. Borin, S. Odenbach, RSC Advances 6 (2016) 100407–100416.
[8] T. Volkova, V. Bohm, T. Kaufhold, JMMM 431 (2017) 262–265.
[9] T.I. Becker, K. Zimmermann, D.Yu. Borin, G.V. Stepanov, P.A. Storozhenko. JMMM, 449 (2018), P 77-82
[10] Borin D.Yu., S. Odenbach, G. Stepanov. JMMM 470, 2019, P. 85-88
[11] Borin, D., Stepanov, G. & Dohmen, E. Archive of Applied Mechanics (2018). P.1-13
[12] G. V Stepanov, D. Yu.Borin, A.V. Bakhtiiarov, P.A. Storozhenko. JMMM, 2019, 498:166125
[13] G.V.Stepanov, D.Yu.Borin, A.V.Bakhtiiarov, P.A.Storozhenko JMMM, 498 (2020) 166071
[14] G. V. Stepanov, D. Y. Borin, A. V. Bakhtiiarov, Smart Mater. Struct., 2020, vol. 30, no. 1
[15] D. Borin and G. Stepanov. Phys. Sci. Rev., 2020, doi: 10.1515/psr-2019-0126.
[16] G. V. Stepanov, D. Y. Borin, A. V. Bakhtiiarov, and P. A. Storozhenko. Phys. Sci. Rev., 2020, vol. 5850, doi: 10.1515/psr-2020-0008.
[17] Borin D.Yu., Stepanov G.V., Dohmen E. (2019) Archive of Applied Mechanics 89, 105-117
[18] Vaganov M., Borin D.Y., Odenbach S., Raikher Y.L. 2020,PhyB..57811866V
[19] Vaganov M., Borin D.Y., Odenbach S., Raikher Y.L. (2019), Soft Matter 15, 4947

Functionalization of biopolymer fibers with magnetic nanoparticles

S. Strassburg, K. Mayer, T. Scheibel

Lehrstuhl Biomaterialien, Universität Bayreuth, Prof.-Rüdiger-Bormann-Str.1, 95440 Bayreuth

Introduction

Fibers made from biopolymers have one benefit over synthetic polymers as they make good scaffolds for embedding nanoparticles without the need of any additional bonding agents. In particular, naturally occurring biopolymers such as proteins exhibit a myriad of interactions with nanoparticles, including ionic, H-bonding, covalent, Van der Waals and electrostatic interactions. The diverse range of interactions between magnetic nanoparticles and biopolymers makes resulting hybrid fibers of particular interest as magnetic responsive materials. Magnetically responsive hybrid biopolymer fibers have many features, including enhanced thermal stabilities, strong mechanical toughness and perhaps most interestingly multi-functionality, allowing for a wide range of applications. These applications range from biosensing, filtration, UV-shielding, antimicrobial and medical applications to name a few.

Production of magnetic particles embedded silk materials

Ongoing work by our group used electrospun meshes of recombinant spider silk protein (based on spider silk proteins derived from *Araneus diadematus*) in hexafluoroisoproponal (HFIP) (Fig 1A) and successfully attached Au coated magnetic nanoparticles to the fiber mesh via dip-coating (Fig 1B) [1]. A high affinity between the recombinant spider silk and the Au magnetic nanoparticles were observed in the fiber meshes. Unfortunately, the low solubility of the Au nanoparticles in the HFIP dope solution prevented electrospinning from a single dope solution. In an effort to circumvent this low solubility, other functionalized magnetic nanoparticles with various shapes and sizes were explored. These included, but are not limited to, hematite iron oxide spindles synthesized by the Wagner group (University of Rostock), bio-phosphate coated magnetite spheres synthesized by the Dutz group (University of Ilmenau) and gelatin-coated nickel magnetic rods synthesized by the Tschöpe group (University of Saarland), all of which were part of the special priority program SPP1681 of the Germen Research Foundation. Each set-up was electrospun into a magnetic mesh to varying degrees of success. The hematite iron oxide spindles did cluster on the spider silk mesh but only sparsely and as large aggregates (Fig 1C) [1]. This is likely due to the low solubility of the hematite iron oxide in the HFIP solutions. The bio-phosphate coated magnetite and gelatin-coated nickel magnetic nanoparticles did show higher solubility in the dope solution but did not adhere to fiber meshes. While not completely solving the issues of solubility, the resulting knowledge from electrospinning a magnetic mesh from a single dope solution did allow for applications developed by [2] Spider silk-magnetic nanoparticle meshes were successfully electrospun onto the surface of self-rolling chitosan films (Fig 1D) [1]. The meshes spun on top did not have an effect on the rolling ability of the chitosan films thus providing a magnetically responsive linning of the inner tube walls.

Outlook

Responsive materials, purification, filtration, antimicrobial properties and bioreactors are but a few of the growing applications for magnetically doped biopolymer composites. The applications for magnetically responsive biocomposite materials will only grow as we learn more about the interaction between biopolymers and nano-

particles. Given the fact that many nanoparticles (and biopolymers) have multiple desired material properties it is likely that literature will start to see more multipurpose materials. With an increase emphasis on biocompatibility, recyclability and "green" environmentally friendly materials, we expect to see a continued shift away from synthetic polymer materials. While still early in development, magnetically responsive biocomposite materials can be used for many applications, and the future looks very promising for their continued study.

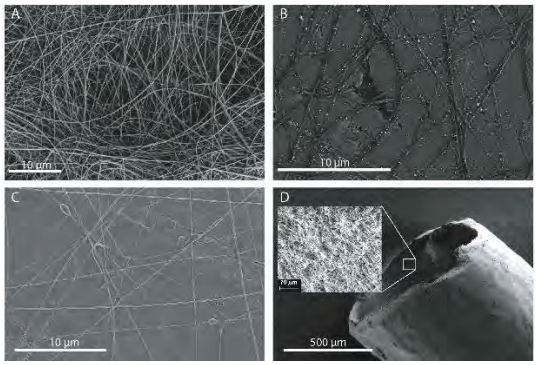

Figure 1. SEM images of electrospun fiber meshes of recombinant spider silk (based on proteins derived from *Araneus diadematus*) (A) without Au coated magnetic nanoparticles and (B) with Au coated magnetic nanoparticles following dip coating. The bright clusters located on the fiber mesh indicate high affinity between the recombinant spider silk and the gold coated magnetic nanoparticles. Because the Au nanoparticles were insoluble in the HFIP solutions, attempts at improving solubility were tested with other coated nanoparticles. The SEM images of electrospun fiber meshes of recombinant spider silk (C) with hematite iron oxide spindles indicate a somewhat successful single pot production of nanoparticle doped spider silk meshes. Building upon these results a recombinant spider silk mesh was applied to a chitosan film. The resulting film indicated no loss of rollability after the mesh was applied (D). The inset of (D) indicates that the electrospun spider silk mesh is present on the inner layer of the chitosan tube. Figure taken from [1].

Acknowledgments

The authors would like to thank the German Research Foundation (DFG) within the priority program SPP 1681.

References

[1] Strassburg, S., Mayer, K., Scheibel, T. Functionalization of Biopolymer Fibers with Magnetic Nanoparticles. Physical Science Reviews, 2020, DOI: 10.1515/PSR-2019-0118

[2] Aigner, T. B., Haynl, C., Salehi, S., O'Connor, A. & Scheibel, T. Nerve guidance conduit design based on self-rolling tubes. Mater Today Bio, 2020. 5: 100042

Field-Induced Deformation of Ferromagnetic Nanocomposites

A. Tschöpe, K. Birster, R. Schweitzer, C. Schopphoven

Universität des Saarlandes, Experimentalphysik, Campus E2 6, 66123 Saarbrücken

Introduction

The incorporation of ferromagnetic particles in a soft-elastic matrix enables remote-controlled shape change of the composite. Torque-induced deformation of textured composites at fields far below the coercivity of the particles can be simulated based on the assumption of hard magnetic dipoles that are fixed to the elastic continuum [1]. However, the anisotropy of any magnetic component is finite, and for fields close to coercivity or even above, the magnetic moments are deflected off the easy axis, which significantly reduces the magnetic torque. As a second aspect, if the matrix material is mechanically compliant, the magnetic particle could rotate by local elastic deformation, which also changes the direction of the moment and feeds back to the torque. The present study aimed to derive and evaluate a microscopic model for the design of shape-changing components, that takes both effects into account. Our approach was closely guided by experiments in which we used hydrogel-based composites with Ni nanorods as the magnetic phase.

Experiments

Ni nanorods were synthesized by the anodic aluminum oxide (AAO) template method and processed to stable colloids [2]. Textured poly-(acrylamide) (PAM) hydrogel nanocomposites were prepared by aligning the nanorods during polymerization [3]. The field- and orientation dependent magnetization and particle rotation were measured using a vibrating sample magnetometer (VSM) and transmission measurements of linearly polarized light, respectively.

Thin filaments of Ni-nanorod/PAM composites were prepared by polymerization in teflon tubes, exposed to a homogenous magnetic field (B = 50 mT) parallel or perpendicular to the tube axis in order to imprint the required texture for bending or torsion experiments. The filaments were fixed at the upper end and the deflection/ rotation of the unconstrained lower end was retrieved from video images. In addition, post-structuring of the magnetic texture by local magnetization reversal was employed for programming of deformation profiles.
Aiming at an increased nanorod volume fraction, composite layers were prepared by magnetophoretic deposition of gelatine-encapsulated Ni nanorods followed by field-induced realignment of the particles and chemical cross-linking.

Results

The reversible magnetization properties of dilute ($\phi_{vol} \approx 10^{-6}$) textured nanorod composites, measured at perpendicular orientation of the texture axis, could be described by a linear superposition of SW-model functions, introducing a density function $P(c_A)$ for the model parameter $c_A = 2K_A/M_s$, with anisotropy constant K_A and saturation magnetization M_s. The extension of the Stoner-Wohlfarth-model (eSW) to include this empirical distribution function as well as the local particle rotation provided a consistent representation of the field- and orientation-dependent torque on isolated Ni nanorods, as confirmed by optical transmission measurements.

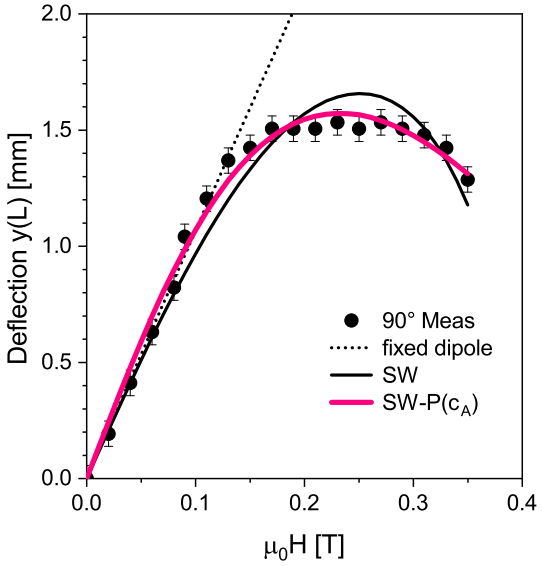

Figure 1: Field-dependent deflection of a textured Ni/PAM filament ($\Theta_0 = 90°$). While the fixed dipole-model was applicable to describe the initial slope, the observed maximum was only revealed by taking the finite magnetic anisotropy (SW) into account. The curvature was well described by including the distribution function for the SW-model parameter, $\mathrm{P(c_a)}$.

Results of bending and torsion experiments on homogeneously textured thin filaments were compared with simulations, based on the eSW-model. The finite anisotropy resulted in a maximum magnetic torque per particle and a corresponding deformation maximum was revealed in field-dependent bending and torsion experiments under suitable conditions, figure 1. Including the distribution of the model parameter $P(c_A)$ was required for quantitative agreement, whereas local rotation apparently played a minor role, which was explained by the cylindrical shape of the Ni nanorods and the resulting efficient mechanical coupling with the matrix.
Controlled local magnetization reversal of the unaxial ferromagnetic nanorods above the switching field enabled reprogramming of the magnetic texture profile and the resulting deformation pattern.

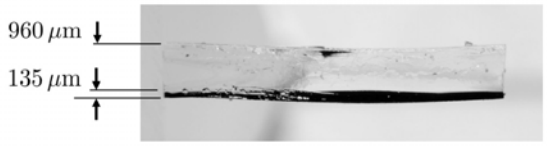

Figure 2: Two-layer composite of a $0.9\,\mathrm{vol.\%}$ textured Ni-nanorod composite (black) and bare glycerol-gelatine hydrogel (transparent).

Increasing the volume fraction of nanorods for potential application faces the challenge of maintaining colloidal stability necessary for homogeneous composites. As a possible strategy, magnetophoretic accumulation of nanorod/gelatine core-shell particles and chemical cross-linking of the glycerol-gelatin matrix was evaluated, figure 2. The nanorod volume fraction in the active layer was increased by two orders of magnitude and the field- and orientation-dependent bending of the two-layer composite was in qualitative agreement with the eSW-model.

Acknowledgments

This work was financially supported by the German National Science Foundation DFG (SPP 1681, grant TS62/4-3)

References

[1] Y. Kim, H. Yuk, R. Zhao, S. A. Chester, and X. Zhao, *Nature* **558** (2018) 274279.

[2] P. Bender, A. Günther, A. Tschöpe, and R. Birringer, *J. Magn. Magn. Mater.* **323** (2011) 20552063.

[3] C. Schopphoven, K. Birster, R. Schweitzer, C. Lux, S. Huang, M. Kästner, G. Auernhammer, A. Tschöpe, *Arch. Appl. Mech.* **89** (2018) 119-132.

Low-cost Magnetic Particle Spectroscopy device for immunoassays

T. Viereck, F. Wolgast, M. Schilling, F. Ludwig

Institut für Elektrische Messtechnik und Grundlagen der Elektrotechnik (EMG), TU Braunschweig, Germany

During the ongoing pandemic, infection control plays an important role. The federal test strategy in Germany relies heavily on antigen quick tests based on lateral flow devices with colloidal gold nanoparticle markers. However, immunoassays using magnetic nanoparticle (MNP) makers can be a fast and quantitative alternative for point-of-need testing. TU Braunschweig has recently established a junior research group to investigate the potential of MNP-based immunoassays for biological testing. Magnetic particle spectroscopy (MPS) provides a fast and highly sensitive tool for measuring the dynamic magnetization response of MNP markers. For that reason, it is particularly suited for magnetic immunoassays.

For testing of infectious samples, we needed a low-cost, fully self-contained, mobile MPS device that could be inserted into a S2+ bio-safety lab. Our newly developed "immunoMPS" is such a device, which delivers high performance (on par or exceeding our lab equipment) for material costs around 300 Euro. The device works with an excitation frequency of 590 Hz in order to capture the Brownian relaxation dynamics of the functionalized MNPs. We are currently working on DNA- and antibody(AB)-based immunoassays. Preliminary results on both strategies have been published [1, 2]. Recent experiments (since early 2021) were performed on the new device. Prime objective was the prototype testing for S1-spike protein of the SARS-CoV-2 virus on patient samples. Currently, we are working towards lower MNP and especially antigen detection limits with an optimized setup and materials.

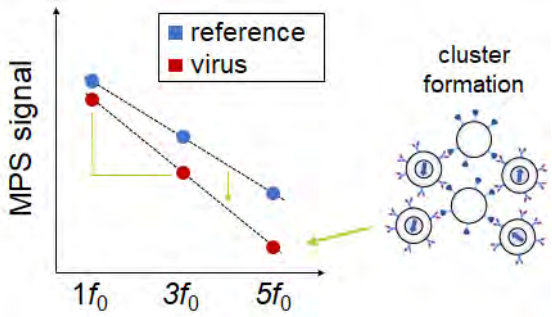

Figure 1. MPS-based virus detection schema

Acknowledgments

DFG: EXC-2123 QuantumFrontiers Germany's Excellence Strategy – 390837967, Research Training Group 1952 Metrology for Complex Nanosystems, ZH 782/1-1.
Niedersächsisches Vorab: Quantum- and NanoMetrology (QUANOMET) initiative projects NL-1 (BL) and NL-2 (TV).

References

[1] Zhong et al., "Toward Rapid and Sensitive Detection of SARS-CoV-2 with Functionalized Magnetic Nanoparticles", ACS Sensors 0c02160 (2021), DOI: 10.1021/acssensors.0c02160

[2] Roesch et al., "Point-of-need detec-tion of pathogen-specific nucleic acid targets using magnetic particle spec-troscopy", Biosens. Bioelectron. 192, 113536 (2021), DOI: 10.1016/j.bios.2021.113536

Goethite Nanorods: Synthesis and how to improve their magnetic properties

M. Weißpflog, S. Hinrichs, B. Hankiewicz

Institute of Physical Chemistry, University of Hamburg, Grindelallee 117, 20146 Hamburg, Germany

Introduction

The majority of research focuses on the ferro- and ferrimagnetism of pure iron, magnetite or maghemite. However, there are also antiferromagnetic species such as goethite that exhibit remarkable magnetic properties. When scaled down to nanometer scale, these naturally anisotropic iron oxide crystals grow into fine needle-shape structures whose orientation depends on the applied magnetic field. Goethite aligns parallel to weak magnetic fields while orienting perpendicular to the field at high field strengths [1]. Furthermore, this iron species is an interesting starting point for an application in minimally invasive hyperthermia techniques, which generate heat under an alternating magnetic field. We assume that the anisotropic properties of goethite will show promising results when combined with a ferro- or ferrimagnetic iron species.

Experimental Section

The synthesis of goethite nanorods was divided into a two-step process. In a first step, we synthesized precursor nanoparticles made of akageneite. These cigar shaped particles are formed by hydrolysis of iron-(III)chloride salts. The transformation of the β-FeOOH precursor into goethite needles were performed under alkaline conditions with NaOH and polyvinylpyrrolidone (PVP) in a hydrothermal reactor at 160 °C and pressurized with nitrogen up to a final pressure of 10 bar. For small particles the addition of the precursor followed the alkaline solution; for larger nanorods the order changed. The subsequent stabilization of the particles in solution was done by adding of PVP and shaking for 2 h.

Results

We synthesized goethite nanorods with lengths between 200 nm and 650 nm. In the standard protocol, we add the PVP prior to the precursor solution at low stirring speeds. This leads to short particles around (210 ± 61) nm in length and (27 ± 9) nm in width resulting in an aspect ratio of 8 (figure 1A). Interestingly, the smallest nano-

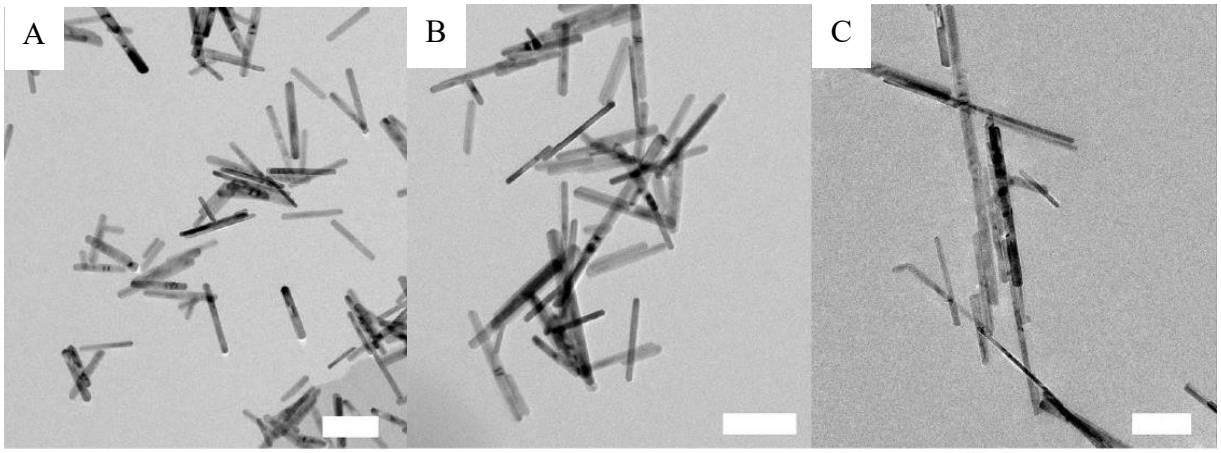

Figure 1. TEM images of selected goethite particles with different synthesis protocols. The scale bar shows 200 nm for the TE micrographs. (A): PVP prior to precursor with small stirring bar. (B): PVP prior to precursor with bigger stirring bar. (C): Precursor prior to PVP with small stirring bar.

rods appear to have the smallest polydispersity of all the samples. By using a bigger magnetic stirring bar, the polydispersity increased (figure 1B). By changing the order of the hydrothermal protocol while adding PVP at last, we produced long (320 nm) particles with an aspect ratio of 13 often accompanied by impurities. The earliest change of the synthesis can be induced by dialyzing the precursor solution resulting in a goethite particle size of about (650 ± 330) nm in length and (32 ± 13) nm in width. Furthermore, the reaction can be easily scaled up, leading to a higher yield, by increasing the precursor concentration. The goethite phase of the samples was confirmed by XRD measurements.

Outlook

For hyperthermia applications, the magnetic properties of goethite need to be improved. The coating of anisotropic goethite rods with magnetite or cobalt ferrite as hard magnetic materials with high coercivity should combine these two features of anisotropy and ferrimagnetism. Along with the hydrothermal synthesis of the magnetic core-shell particles as nano-heating elements, high saturation magnetisation values should be achieved. First biocompatible experiments were carried out in a precursor-based process and showed a doping of the goethite surface. These composites with magnetic anisotropy promise to have potential application in the field of sensor technology and hyperthermia.

Acknowledgments

The authors acknowledge the Deutsche Forschungsgemeinschaft (DFG) via the priority program SPP 1681 "Feldgesteuerte Partikel-Matrix-Wechselwirkungen" Grand Nr. Fl 1235/2-2. The authors gratefully acknowledge A. Barck and M. Fritz for measuring XRD.

References

[1] Hinrichs, S.; Grossmann, L.; Clasen, E.; Klages, H.G.G.; Skroblin, D.; Gollwitzer, C.; Meyer, A.; Hankiewicz, B. Goethite nanorods: Synthesis and investigation of the size effect on their orientation within a magnetic field by SAXS. *Nanomaterials* **2020**, *10*, 2526-2537.

Influence of sheep blood on the magnetoviscous effect of biocompatible ferrofluids

C. Wermann[1], S. Odenbach[1]

[1] *Chair of Magnetofluiddynamics, Measuring and Automation Technology, Technische Universität Dresden, Georg-Bähr-Straße 3, 01062 Dresden*

Introduction

Until today cancer is one of the leading causes of death worldwide. In 2020 nearly 10 million people died from the disease. Projections show, that the number of deaths due to cancer will continue to increase [1]. Therefore there is great interest in magnetic nanoparticles (MNP) to complement traditional therapies like chemo- or radiotherapy. To ensure a safe application of MNP, it is necessary to fully understand their behaviour in the human body. This knowledge has not yet been achieved. Johannes Nowak discovered in his research that ferrofluids show a greater magnetoviscous effect (MVE), if they are diluted with sheep blood, compared to ferrofluids diluted with water [2]. He suggests, that this phenomenon results from an interaction between the MNP and the blood. The purpose of this work is to replicate this effect and to investigate if the interaction takes place between the MNP and specifically the red blood cells (RBC).

Methods

In the first step the rheologic, magnetic and magneto-viscous properties of the selected ferrofluid fluidMAG-D200 (chemicell GmbH, Berlin, Germany) were examined. Subsequently the rheologic properties of the sheep blood, blood plasma and multiple suspensions with increased hematocrit value (Hct) were determined. In the main study, the MVE of the ferrofluid, diluted with sheep blood, water, blood plasma as well as two suspensions with $Hct = 50\,\%$ and $Hct = 100\,\%$ was measured. The dependency of the MVE on the shear rate and the magnetic field strength was determined. A relevant parameter is the maximal MVE as well as the MVEs reduction over the shear rate. A Physica MCR 301 rheometer (Anton Paar GmbH) was used to determine the rheological properties of the samples. A special shear rate controlled rheometer for magnetic fluids [3] was used to measure the MVE.

Results

In this study no increased MVE was observed for fluidMAG-D200 diluted with sheep blood compared to water as dilutant. Therefore, the effect could not be replicated. Furthermore, no significant reduction of the MVE was found in the suspensions with increased RBC concentration. Even the progression of the MVE over the shear rate did not change significantly with rising Hct.

Conclusion

These results do not confirm the increased MVE in ferrofluids diluted with sheep blood which Nowak observed in his study. This deviation can possibly be explained by the viscosimeter used. In this study a rotational rheometer was used, while Nowak conducted his experiments with a capillary viscosimeter. Moreover the

range of the field strength in the capillary viscosimeter extends from $H = 30\,\mathrm{kA\,m^{-1}}$ to $H = 350\,\mathrm{kA\,m^{-1}}$, while the rheometer for magnetic fluids can only be operated up to $H = 35\,\mathrm{kA\,m^{-1}}$. Possibly, the increased MVE of the ferrofluid diluted with sheep blood will only take place at field strengths $H > 35\,\mathrm{kA\,m^{-1}}$. In addition the flow situation in a capillary tube differs from the flow situation in a cone-plate-geometry and could therefore affect the behaviour of the ferrofluid and the sheep blood.

References

[1] *Cancer*, WHO, 2021, URL: `https://www.who.int/news-room/fact-sheets/detail/cancer`

[2] J. Nowak, „Magnetoviskose Effekte blutverdünnter Ferrofluide“ (German) [Magnetoviscous effect of ferrofluids diluted with blood], Diss. faculty of mechanical engineering, Technische Universität Dresden, 2016

[3] S. Odenbach and H. Störk, „Shear dependence of field-induced contributions to the viscosity of magentic fluids at low shear rates“ *J. Magn. Magn. Mater.*, 1998, *183*, 188

Magnetic multicore nanoparticles for drug targeting to the eye

D. Zahn[1], K. Klein[1], P. Radon[2], E. Nagel[1,3], M. Eichhorn[4], F. Wiekhorst[2], S. Dutz[1]

[1] *Institute of Biomedical Engineering and Informatics, Technische Universität Ilmenau, Ilmenau*
[2] *Physikalisch-Technische Bundesanstalt, Berlin*
[3] *Ophtalmic Practice, Rudolstadt*
[4] *Institut für Anatomie, LSII, Universität Erlangen-Nürnberg, Erlangen*

Introduction

Conventional strategies for applying drugs into the eye are faced with several problems, like discomfort for the patient in case of injections and a limitation of the drug concentration inside the eye for systemic administration. To avoid these drawbacks, new approaches for drug targeting to the eye would be beneficial. Therefore, this paper elucidates the feasibility of magnetic drug targeting to the eye by using magnetic multicore nanoparticles (MNP) as vehicles for pharmaceutical agents, transported through the eye tissue by means of a magnetic field gradient.

Methods

Optimized magnetic nanoparticles for application in drug targeting were synthesized with a co-precipitation method. To achieve a so-called multicore structure of the particles, the alkaline medium ($NaHCO_3$) was added slowly over a period of 15 minutes to the iron salt solution ($FeCl_2$ and $FeCl_3$). Resulting precipitate was heated to 100°C to evaporate CO_2 and transfer it into the magnetic phase magnetite/maghemite followed by magnetic washing. The MNP were coated with several materials (starch, carboxymethyldextrane CMD, dextrane DEX, citric acid CA, polyethylenglycol PEG and trisodium citrate NaZ) via an adhesive coating process to achieve stable aqueous suspensions and assure bio-compatibility.

The MNP were characterized using TEM, DLS, zeta-potential measurements, XRD and VSM concerning their structural and magnetic properties.

To evaluate the stability of the used coating materials in biological fluids, turbidimetry measurements using UV/VIS spectrometry were made with three different media: ultrapure water for injections, physiological NaCl solution and artificial tears fluid.

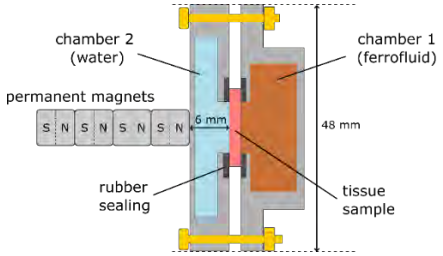

Figure 1. Scheme of the lab setup for targeting experiments.

Next, a setup was designed to evaluate the magnetically driven passage of particles through samples of eye tissue (see fig. 1). Sclera and cornea samples were harvested from domestic pig eyes and placed as a separator in a 3D-printed two-chamber-setup. Chamber 1 is filled with the MNP suspension, chamber 2 with deionized water. Since previous numerical simulations revealed that a gradient of 20 T/m seems to be promising to drag MNP through eye tissue, a combination of permanent magnets was used to generate this gradient for the experiments. The magnets were placed on the wall of chamber 2, so particles were pulled from chamber 1 through the tissue sample to chamber 2. Resulting MNP concentration in chamber 2 was evaluated using MPS, which quantifies the content of iron in MNP using the amplitude of the third harmonic A_3 of the measured spectrum. Each combination of particle coating and tissue was tested several times with and without a gradient as a control.

Results and discussion

Structural characterization of the uncoated particles confirmed the multicore structure. XRD measurements show a size of the individual cores of about 13.6 nm, confirmed by TEM images with resulting core sizes of 12 – 14 nm and a cluster size of about 45 nm. In VSM measurements, the dried powder of bare MNP show a ferromagnetic behavior with a saturation magnetization of 72.9 $Am^2/kg_{(MNP)}$, a coercivity of 1.59 kA/m and a relative remanence of 0.04.

Coated particles exhibit hydrodynamic diameters in DLS between 130 nm (NaZ) and 296 nm (starch). Starch leads to a matrix like structure with embedded MNP, rather than individually coated particles, which explains the increased hydrodynamic diameter. This is confirmed by VSM measurements of the coated particles, where after starch coating M_S decreased down to 54 $Am^2/kg_{(MNP)}$, indicating a thick non-magnetic layer of starch around the magnetic particles. In comparison, NaZ coated particles show the smallest hydrodynamic size and a high M_S of 70.1 $Am^2/kg_{(MNP)}$, as a consequence of a thinner coating layer.

In turbidimetry experiments, starch coated particles were found to be stable in all three media over a period of 24 hours. DEX also shows promising results, while all other coatings lead to instant sedimentation in NaCl solution and a slower, but none the less significant sedimentation in artificial tears.

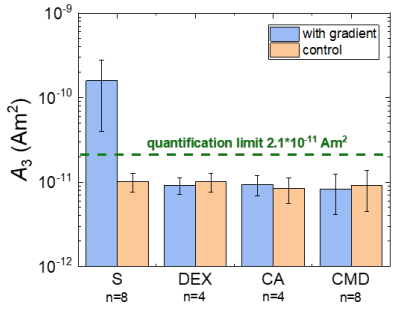

Figure 2. Third harmonic A_3 of 30 μl samples from chamber 2 for all coatings tested with sclera tissue measured by MPS.

Targeting experiments showed that no particles were able to penetrate cornea tissue, but starch coated MNP could pass sclera samples with a rate of 5.4 ± 4.1 ng/mm (average of 8 experiments, each one taking 24 h), see fig. 2. Despite the large standard deviation, this is a very promising result, since in each of the 8 experiments with starch and sclera a significant amount of MNP was found in the target chamber, while no MNP signal was measured in all other combinations.

Conclusion and outlook

In this work, we report the first successful targeting of magnetic multicore nanoparticles through eye tissue, driven by magnetic field gradients. We synthesized optimized MNP with a high M_S of 73 $Am^2/kg_{(MNP)}$ and a low H_C and M_R at the same time. Starch turned out to be the most promising coating material for biological applications, shown by superior stability in biological fluids and confirmed by successful targeting experiments. Only starch coated particles were able to penetrate sclera samples with a rate of 5.4 ng/mm, while all other coatings could not pass the tissue. Although the amount of particles detected in the target chamber is rather low, our findings open the door for drug targeting to the eye using magnetic particles as drug carriers, placing them outside of the eye and dragging them into it magnetically.

Acknowledgements

This work was supported by the “Thüringer Innovationszentrum für Medizintechnik-Lösungen” (ThIMEDOP; FKZ IZN 2018 0002) and by the Freistaat Thüringen (contract 2016 FE 9100) and is co-financed by the European Union in the frame of the ‘European Regional Development Fund (ERDF)’. Funding was provided by the DFG core facility, grant numbers KO5321/3 and TR408/11 for the MPS quantification measurements. The authors thank the Mühlhäuser Fleisch GmbH (Mühlhausen, Germany) for providing the animal tissue samples.